University of Cambridge
Department of Engineering

Cover elements for retractable roof structures

First-year report submitted to the University of Cambridge
on the progress of Ph.D.-work

by

Frank Vadstrup JENSEN

Darwin College

November 2001

Acknowledgements

The research work described in this report was carried out by the author at the Department of Engineering, Deployable Structures Group, at the University of Cambridge from January 2001 to November 2001. The work was carried out under the supervision of Professor *Sergio Pellegrino* and financed by Søren Jensen Rådgivende Ingeniørfirma as.

Firstly, I would like to express my gratitude to my supervisor Professor *Sergio Pellegrino* for his scientific guidance and valuable advise.

I also thank my advisor Professor *C. R. Calladine, FRS,* for his scientific advice on my work.

I would also like to express my gratitude to all the members of the Deployable Structures Group and Structures Research Group, especially Dr. *Elizbar Kebadze*, *Lars Ekstrom* and *Andrew Lennon*, for their invaluable advice, help and friendship. I am also grateful for the very constructive discussions with Civilingeniør *Thomas Buhl*, of the Technical University of Denmark, and for his friendship.

Finally, I am grateful for the support I have received from my sponsors Søren Jensen Rådgivende Ingeniørfirma as. Especially from Director *Erik Jensen* whom as my father and tutor have given me immense support.

Cambridge, November 2001

Diplomingeniør *Frank Vadstrup Jensen*

Declaration

The author declares that, except for commonly understood and accepted ideas, or where specific reference is made to the work of other authors, the contents of the report are his own work and include nothing that is the outcome of work done in collaboration. This report has not been previously submitted, in part or in whole, to any University or Institution for any degree, diploma or other qualification. This report is presented in 66 pages and contains approximately 12,000 words, including bibliography.

Diplomingeniør *Frank Vadstrup Jensen*

Abstract

Over the last decade many large scale stadia have been developed and built across the world. This trend is set to continue as sporting events and tournaments such as the Olympics require the provision of modern venues. There is therefore a need for continuously developing and improving the design for these large venues. Many modern venues require the spaces to be multi-purpose to increase revenue and a popular method of achieving this is by adopting a retractable roof structure.

This report presents some new solutions for the design of novel retractable roof structures. The work presented is based on an existing type of circular bar structure which forms a series of interconnected rhombuses and that is capable of retracting towards the outer boundary of the structure.

By analysing the motion of this type of bar structure a method is derived for finding simple rigid shapes that can be attached to the bar structure and which do not interfere with each other when the structure moves. An analytical solution for the shape of these rigid cover elements is derived.

The cover elements forms, i.e. gap free, surface in both the open and closed position. The shape of these elements is basically triangular, but a number of features – which need to fulfill certain conditions of periodicity – can be incorporated. For example it is possible to chose a shape consisting of circular arcs such that a perfectly circular opening is obtained when the structure is retracted.

If certain geometric conditions are fulfilled, the joints of the bar structure fall within the covering elements, in which case the bar structure is no longer needed and the whole structure can be made from rigid plate elements alone.

Two physical models of these plate structures have been made to demonstrate some of these new solutions.

A unified design method for both types of structures is proposed in the report.

Contents

List of Figures

Chapter 1

Introduction and Review of Literature

1.1 Background

Over the last decade many new stadia and other large outdoor arenas have been built around the world. The construction of many of these has been driven by the hosting of large sporting events such as the Olympic Games or European or World Championships in football. However these events are usually only one off events and thus do not form the basis of the cost-benefit analysis, which must be carried out to justify the large investment required for such structures. Instead, revenues are generated by hosting various events. It is therefore an integral part of any feasibility study for such structures to try to quantify benefits that can be derived from increased flexibility of structures which cannot only perform as outdoor venues but also as indoor venues. Therefore, some of these new stadia have been constructed with retractable roofs in an attempt to guarantee higher and revenues. In America the larger construction costs of retractable roof structures have often been found to be viable, as opposed to Europe where stadia traditionally have been pure outdoor arenas for sports such as football and athletics.

The number of such structures has rapidly increased and it is likely that this trend will continue in the near future as the need for large venues especially in Europe and Asia has yet to be saturated. As a response to this demand designers and builders are developing new systems and methods for construction of these structures and also retro-fitting older structures with retractable roofs.

All these projects are however carried out in an economic environment that requires the support of public authorities. This is because the venues at present cannot generate sufficient revenue and profits to make them viable without such support [3, 11].

This report describes the progress of research into a novel structural system,

which can be applied to retractable roofs for large span structures.

1.2 Review of Literature

A large number of structural systems have been proposed in the past and are currently used for retractable roof structures. These range from heavy concrete shells to light membrane structures. The purpose of these structures is to provide enclosures for a wide variety of activities such as sporting, conference, music and performing arts events. It is a response to this wide variety of uses that retractable roofs have been developed and found in some cases to be economically more attractive.

Retractable roofs have been around for a long time. Large scale awnings were used by the Romans to cover the spectators at their amphitheatres from the rain and sun. Other early examples are simple umbrella-like structures, which were much later followed by foldable membrane structures on a large scale, and rigid retractable structures [2].

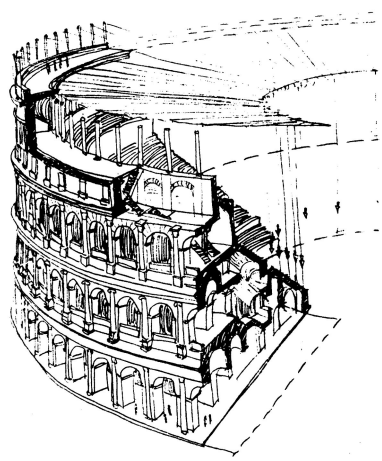

Figure 1.1: Coliseum in Rome [2]

The ingenuity of the designers of these structures has led to a very wide range of solutions and as retractable roof structures have become more common and conventional, papers and design guides have been published. These deal with issues ranging from planning and architecture to driving mechanisms and loads. Figure 1.2 shows various examples of these systems [1, 6].

As an introduction to the theme of retractable roofs and to the scheme presently being researched a number of projects is presented briefly.

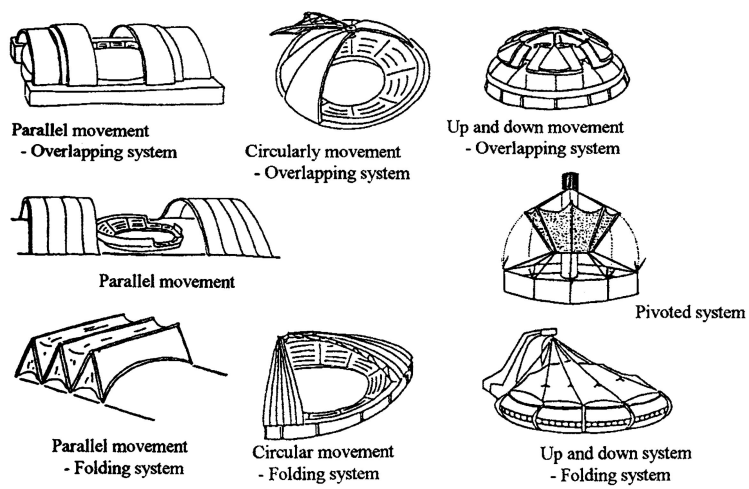

Figure 1.2: Various retractable roof systems [2]

1.2.1 Ball Dome (Japan)

The roof of this structure is made from two separate layers of arched steel trusses and dual membrane covers and spans 37 meters. To retract the roof first the inner layer rotates 90° so it overlaps the outer layer, in this position the roof covers approximately 60% of the initially covered area. This motion is controlled by a curved rail along the perimeter of the roof. To completely open, the entire roof is moved sideways along a different set of rails. To allow for the rotational movement a clearance of 250 mm is present between the two layers. To prevent rain and wind penetration into this void an inflatable tube is placed between the layers [6].

1.2.2 Fukuoka Dome (Japan)

The 222 m span Fukuoka Dome is covered by three large roof panels. These are made from steel trusses and are individually able to withstand the forces that are imposed on them. This is done by letting each panel subtend a horizontal angle of nearly 180° at the base, thus making the panels stable individually. At the centre of the span the three panels are connected via a large cylindrical joint. To ensure clearance between the panels there is a 1.7 m distance between the panels at the central joint. Here the panels only cover an angle of 125° each. The inner panel is fixed to the permanent structure but the two outer layers are rotated about the centre of the structure and are supported by bogies along the circumference of the structure [6].

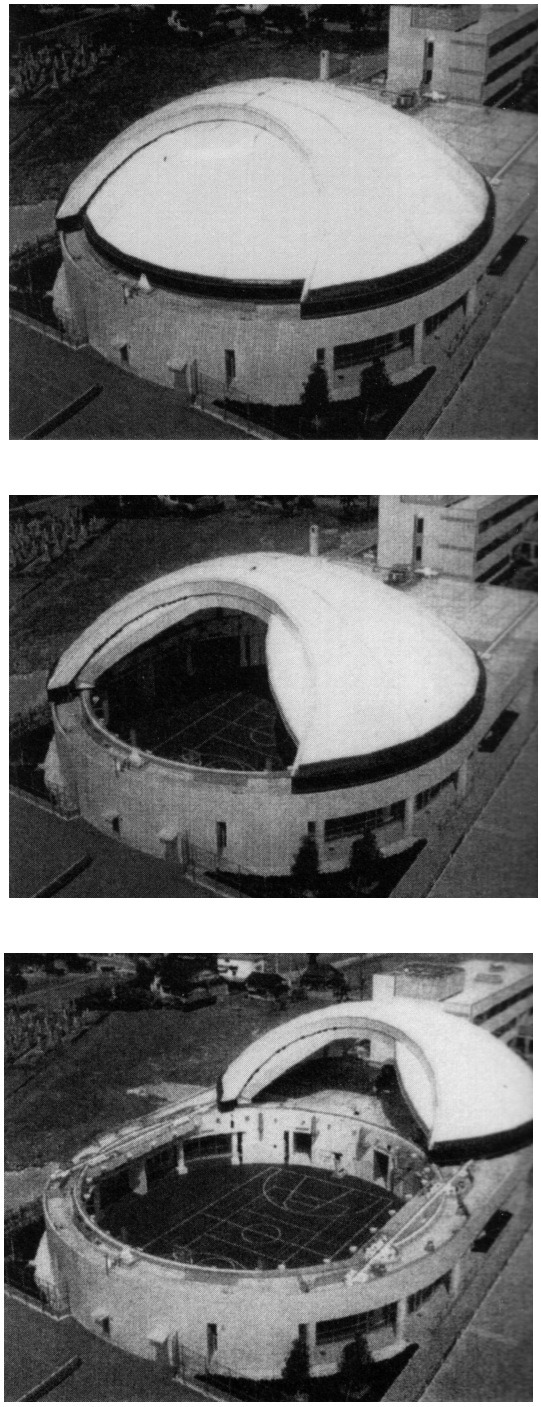

Figure 1.3: Opening of the Ball Dome [6]

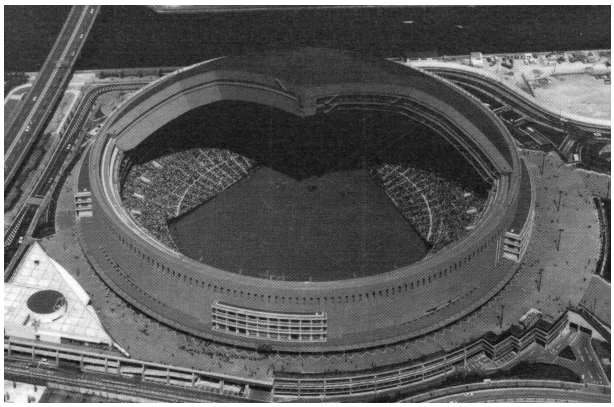

Figure 1.4: Fukuoka Dome [6]

1.2.3 The Millennium Stadium (UK)

This 72,500 capacity stadium uses two rigid roof sections to cover the 120 m × 80 m opening. These sections are each made of a series of trusses and a flat roof deck of insulation clad aluminium sheets. This was done to allow for an acoustic performance of the enclosed space which can provide good facilities for indoor concerts. The two sections run on rails that are fixed to the permanent structure. To simplify the mechanical system, the retracting sections are controlled and powered through cable loops by motors and gearboxes fixed to the permanent structure [1].

1.2.4 Vista Alegre (Spain)

Here an existing structure was fitted with a light membrane cushion to cover the central bull-fighting area. The cushions are made from Polyester/PVC for the upper face and a cable reinforced ET transparent membrane for the lower face.

The cushion has a diameter of 50 m and can be lifted 11.4 m using columns and winches. The assembly is fixed to the existing cantilevering roof over the grand stand. The roof was extended in order to provide sufficient cover for the audience throughout the season [1].

1.2.5 Olympic Stadium in Montreal (Canada)

This Olympic stadium had its folding membrane roof replaced after it was damaged by local failures due to aero-elastic instability occurred several times during opening and closing. The 20,000 m^2 opening was originally covered with a PVC/Kevlar membrane but was replaced with a non-retractable cable stayed

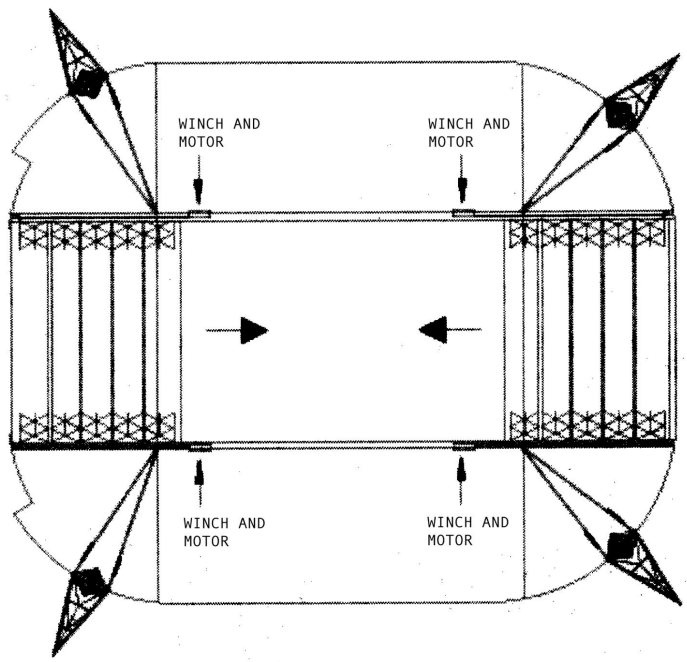

Figure 1.5: System for retraction of the Millennium Stadium roof [1]

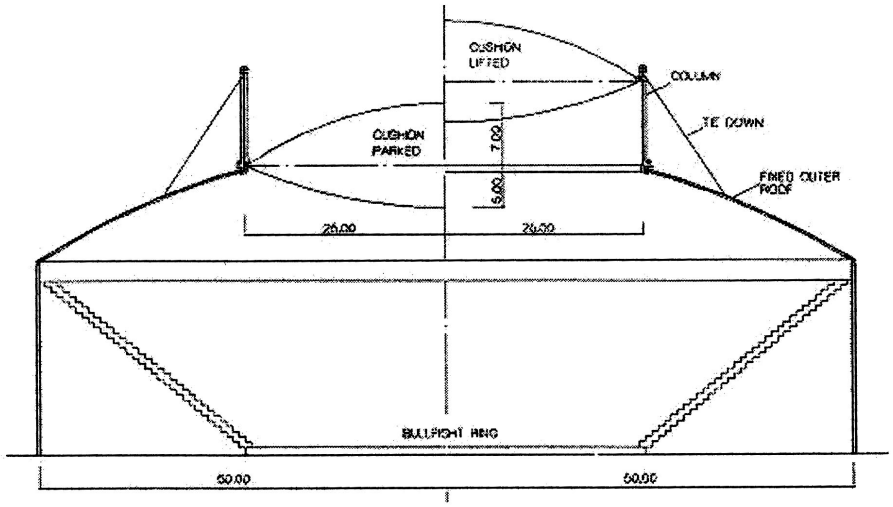

Figure 1.6: System for opening roof over the Vista Alegre bull fighting ring [1]

spatial steel framework. The original membrane roof could be retracted along a number of cables for stowage, see Figure 1.7 [1, 6].

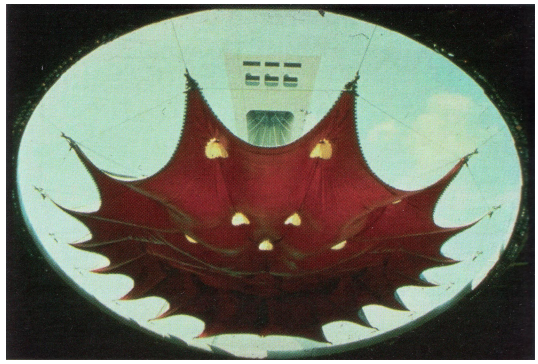

Figure 1.7: The original membrane roof on the Montreal Olympic Stadium [1]

1.2.6 Retractable Structures using *Scissor Hinges*

These structures were largely pioneered by the Spanish engineer Pinero and have been further developed by Escrig and Zeigler [8].

A large number of structures that can be opened and closed are based on the well know concept of *scissor hinge* system. The scissor hinge or cylindrical joint allows one relative rotation, about is own axis, between connected members while other relative rotations and translations are inhibited. These hinges allow structures to be made so that they can be compacted using the principle of the lazy-tong. This type of structure has been used by designers to construct many demountable structures, some of which could be classified as retractable roofs though they require manual intervention for opening and closing. A considerable problem for structures that make use of scissor hinges is how to connect to a permanent foundation.

One major advantage of these structures is the relative simplicity of the joints, compared to other deployable structures.

1.2.7 The Iris Dome

The American engineer Hoberman made a considerable advance in the design of retractable roof structures based on scissor hinges when he discovered the simple *angulated element* [4]. This element consists of two identical angulated bars connected together by a scissor hinge at node E, see Figure 1.9, and forms the basis of a new generation of retractable structures.

This element is able to open and close while maintaining the end nodes A, B, C, D

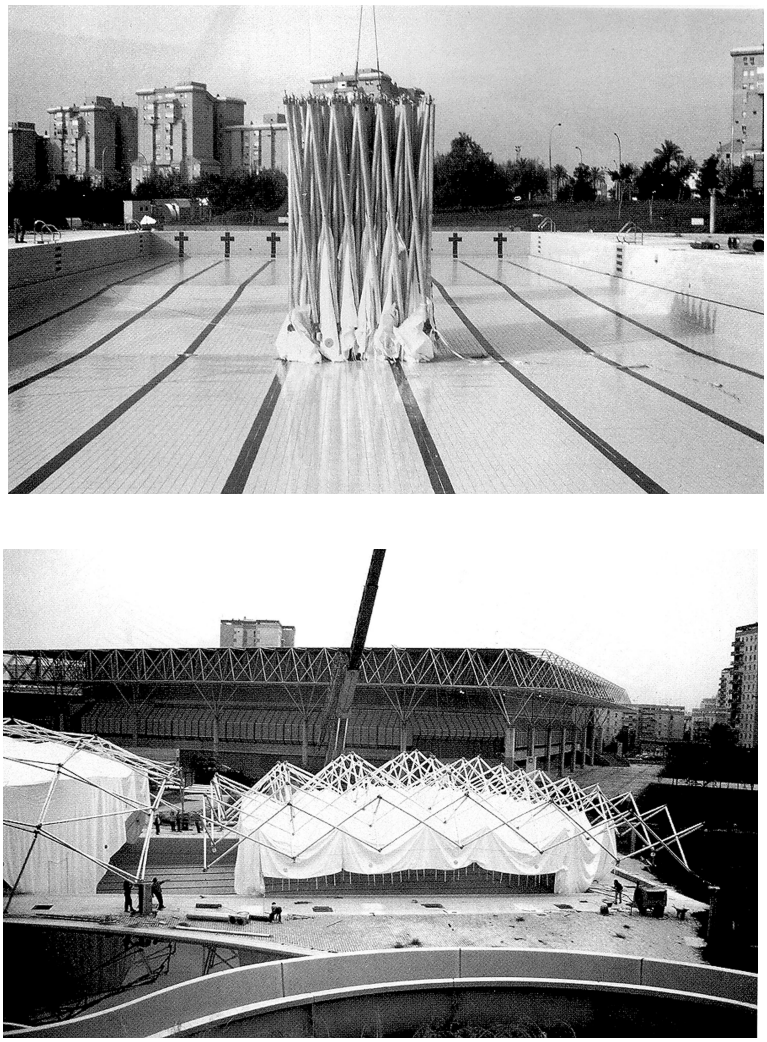

Figure 1.8: Deployment of Escrig's deployable roof structure [8]

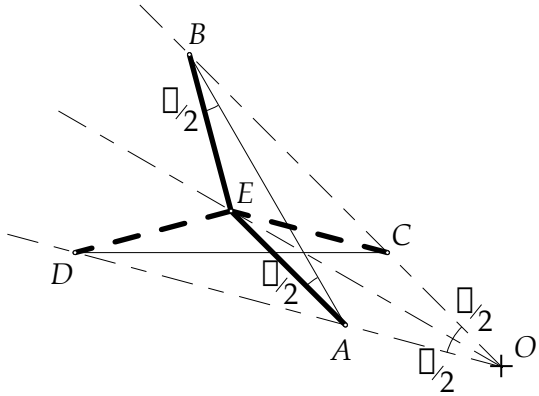

Figure 1.9: Angulated element

on radial lines that subtend a constant angle. Using these elements Hoberman created the retractable roof of the Iris Dome, shown in Figures 1.10 and 1.11, and other foldable structures [5, 13].

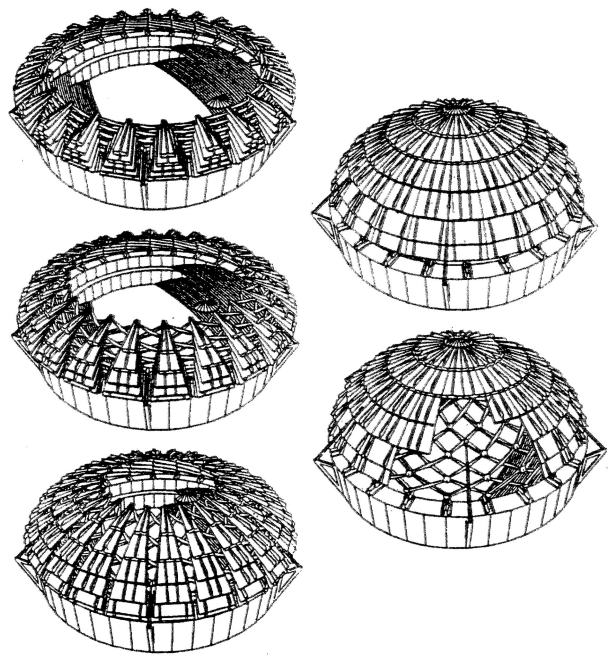

Figure 1.10: Iris Dome [8]

The Iris dome is constructed from a number of angulated elements arranged on concentric circles. These form in plan a circular shape and the circles are connected to each other by joints connecting the end nodes of the angulated elements, creating a series of pin-jointed parallelograms. This allows the structure to retract towards its perimeter thus creating a central opening at the centre when retracted. This structure, however does not maintain a constant perimeter and thus problems with the connection to the foundation persists. However, as the change of radius at the boundary of the structure is much smaller than for previous structures, the scale of the problem has been reduced and several small scale Iris domes have been built, such as the one shown in Figure 1.11.

An enclosure can be created by covering angulated elements with rigid plates which are allowed to overlap in the retracted position. Several different designs have been proposed by Hoberman [5]. The Iris Dome consists of a large number of plates and bars, and requires many hinges. This can causes potential problems with reliability and at present no large scale structure has been built using this system.

Figure 1.11: Iris dome at EXPO 2000 in Hanover, Germany

1.2.8 Multi-Angulated Elements

Further progress on this type of structures was made possible by the discovery by You & Pellegrino of using so-called *multi-angulated elements*. Each multi-angulated element is composed of a number of bars, which are rigidly connected to each other, instead of separate angulated elements as used by Hoberman. Retractable structures made from two layers of such elements connected only by cylindrical joints are shown in Figure 1.12. The two interconnected layers create a series of rings, each consisting of a ring of rhombuses.

An entire family of these structures has been identified; they all have the ability to retract radially towards the perimeter and can be generated for any plan shape. This makes them particularly interesting for sporting venues where retractable roofs must be able to retract towards the perimeter of the structure [2, 10, 13].

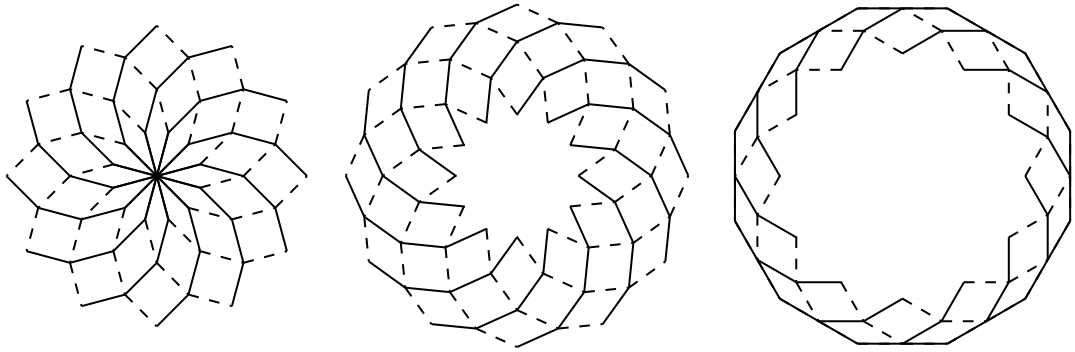

Figure 1.12: Deployable structure using angulated elements

However, the system has only been made to work for motion in a plane. To design practical structures any solution that would work in *two* dimensions, can be projected vertically onto a 3-dimensional surface. Such a structure is shown

in Figure 1.13. As the perimeter of the structure varies during retraction the support conditions need to allow this motion. A possible solution, where the structure is mounted on pinned columns, is demonstrated by the model shown in Figure 1.13. Further work on support conditions by Kassabian showed that, if a rigid body rotation of the structure is allowed, then the motion of each angulated element is a pure rotation about a fixed point and hence can be described by a circle. Therefore it is possible to support the structure on a number of fixed points each corresponding to the centre of one of these circles. This has been demonstrated by Kassabian & Pellegrino [7, 8].

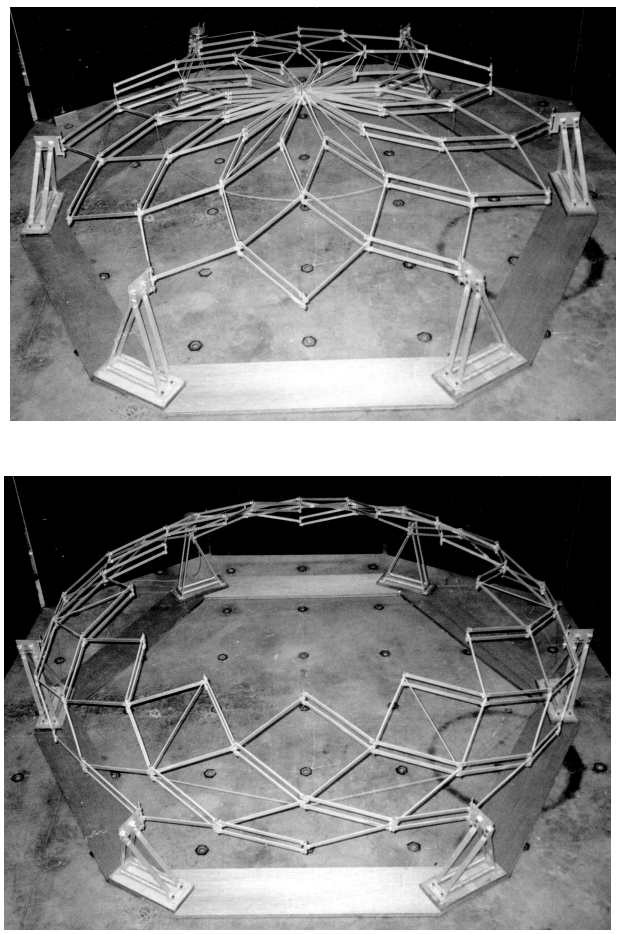

Figure 1.13: Deployable "spherical" structure using angulated elements

The geometry of this type of structures is determined by the length of each bar forming the angulated elements, l; number of bars in each angulated element, k, and number of segments, n. The number of segments is equal to the number of angulated elements in each layer of the structure. These variables are defined in Figure 1.14. From these variables, the radius of the circle, $r^\star$, describing the

motion of the angulated elements can be determined [2, 10, 13]:

$$\alpha = \frac{2\pi}{n} \tag{1.1}$$

and

$$r^{\star} = \frac{l}{2\sin\frac{\alpha}{2}} \tag{1.2}$$

It will later prove useful to define the radius of the circle instead of starting from the length of the bar, which in turn can then be found from Equation 1.2. Also as only a single length defines the whole structure, all elements can be scaled linearly. Therefore, all dimensions in the following will be non-dimensionalised by dividing by the radius, $r^{\star}$. Thus, the *configuration* of a structure is defined by only two parameters n;k.

The kink angle – which os the same for all scissor joints – is α, see Figure 1.14.

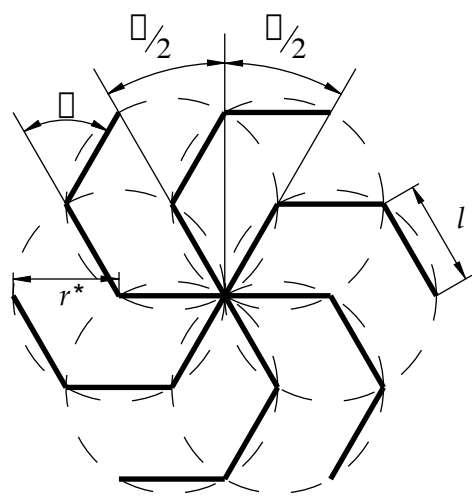

Figure 1.14: One layer of structure with configuration 6;3

1.2.9 Cover plates

Kassabian [7] suggested that to provide a retractable roof using this type of structure, a series of rigid cover elements used should be attached to the multi-angulated elements, instead of using membranes which repeatably fold and unfold. The shape of these cover elements should be such that they do not interfere nor overlap during motion. They should also provide a continuous, i.e. gap

free, covering surface in both the open and closed positions of the structure. Using a kinematical approach, two possible designs were developed. Each cover is attached to a single angulated element so the motion of the structure is not inhibited [7, 8].

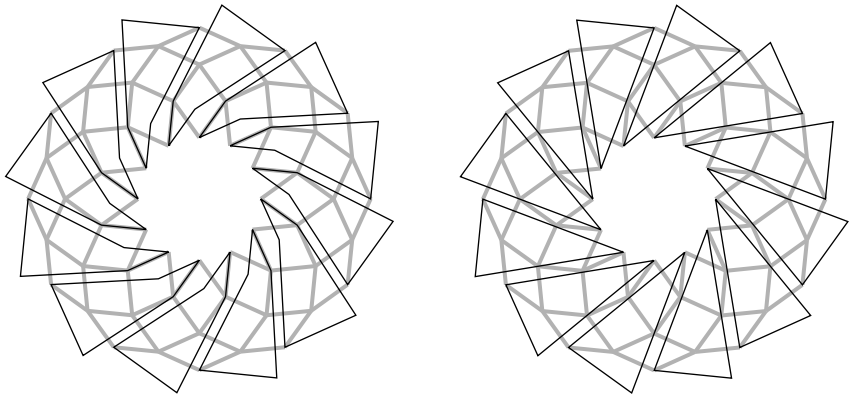

Figure 1.15: Previous covers for deployable structure

1.3 Aims and scope for this study

The current research aims at developing a novel type of retractable roof structure that could be used for covering large venues such as stadia. This report provide an overview of the work carried out to date.

The research carried out so far has been focused on developing an understanding and description of the behaviour of the *two*-dimensional bar structure. This has in turn led to the derivation of a unified approach to the design of flat rigid cover elements.

By considering the motion of the overall bar structure and parts thereof, a method for finding shapes of the cover elements which satisfy the design criteria is presented. This method and findings using this method are described in the report.

It is also shown that this method can be used for designing two different types of structures. The first structure is a bar structure covered, as initially proposed, by rigid elements. The second structure consists of two layers of plate elements connected through cylindrical joints, which executes the same motion as a similar bar structure. The design of both types of structures is described in the report.

The report is concluded by a discussion of the results presented and an outline of future work that is planed.

1.4 Layout of Report

In Chapter 2, two methods for describing the motion of the bar structure are introduced. These have been developed to take account of practical issues such as finite size of the elements and joints. The results are presented in design charts that can be used for designing structures made from multi-angulated elements.

In Chapter 3 it is shown, by considering the bar structure as a series of interconnected parallelograms, that it is possible to cover the structure with rigid elements so that these do not restrict the motion of the structure. The basic shape of these cover elements is found to be governed by the overall configuration of the structure.

In Chapter 4, some changes to the basic shape of the cover elements are shown to be possible. Again, considering the motion of a parallelogram, a set of rules that allow a number of changes are derived.

In Chapter 5, the findings of the research are presented as a simple guide for future designers of these structures. Though the guide is not exhaustive, it provides an overview of the method described in the report and examples of its application. Two different types of structures are covered.

In Chapter 6, the conclusions for the research carried out to date are stated and a future course of the research is suggested based on a discussion of the results presented.

Chapter 2

The Basic Bar Structure

The motion of a circular structure consisting of identical angulated elements can be described using two different methods, depending on whether the structure expands radially without rotation or each angulated element moves along a circular path. Thus, there are two different measures, length and angular rotation, when describing the motion of the structure. This chapter presents methods for comparing the motion of various configurations of bar structures.

2.1 Radially Expanding Structure

Describing the motion of the bar structure as radially expansion, there will be two extreme positions, the *open* and *closed*. The closed position is defined when the structure has the minimum possible distance between the origin, O, and the innermost node of the angulated elements. This distance is called r_{min}. Similarly the open position is defined when the distance has the maximum length and is denoted r_{max}. The open position is reached when the outer ring of rhombuses in the structure have been distorted to the point two diagonally opposite joints coincide and further motion is impossible. The distance to the outer boundary is also defined for both the open and closed positions as R_{min} and R_{max}. These are shown in Figure 2.1 where R_{min} is equal to *zero*.

To compare the motions of various configurations three ratios are introduced. The opening ratio, OR, is defined as the radius of the central opening in the open position, r_{max}, divided by the outer radius of the structure in the closed position, R_{min}. $OR < 1$ indicates that there is an overlap between the two positions, which can be used when considering various methods for supporting the structure.

The second ratio is the stowage ratio, SR. This is defined for the open position only and is defined as the outer radius, R_{max}, divided by the radius of the opening,

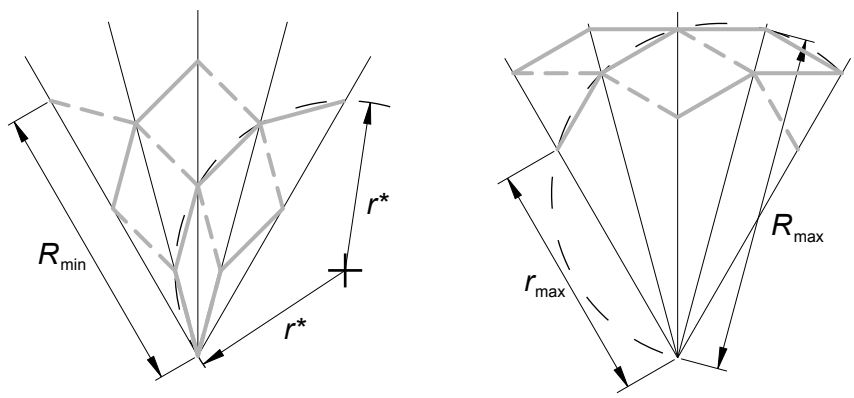

Figure 2.1: Dimensions for the open and closed positions

r_{max}. It indicates the size of the central opening compared with the maximum, outer size of the structure. It describes the stowage efficiency of the structure.

It is of interest to compare SR with the best possible, which is $k = 2$. Thus $SR^\star$ is defined and is the third ratio that will be introduced.

To calculate the ratios defined above the various radii are calculated for an arbitrary structure, defined by the configuration of n and k. All the equations have been written in terms of $r^\star$ – recall that this is the radius of the circle describing the motion of each angulated element. Details of the derivation are not given, but a similar derivation is shown in Section 2.3.

$$R_{\max} = 2r^\star \tag{2.1}$$

$$R_{\min} = 2r^\star \sin\left(k\frac{\pi}{n}\right) \tag{2.2}$$

$$r_{\max} = 2r^\star \cos\left((k-1)\frac{\pi}{n}\right) \tag{2.3}$$

The ratios OR, SR and $SR^\star$ can thus be derived:

$$OR = \frac{r_{\max}}{R_{\min}} = \frac{\cos\left((k-1)\frac{\pi}{n}\right)}{\sin\left(k\frac{\pi}{n}\right)} \tag{2.4}$$

Equation 2.4 is plotted as a function of n and k in Figure 2.2.

The expression of SR is:

$$SR = \frac{R_{\max}}{r_{\max}} = \frac{1}{\cos\left((k-1)\frac{\pi}{n}\right)} \tag{2.5}$$

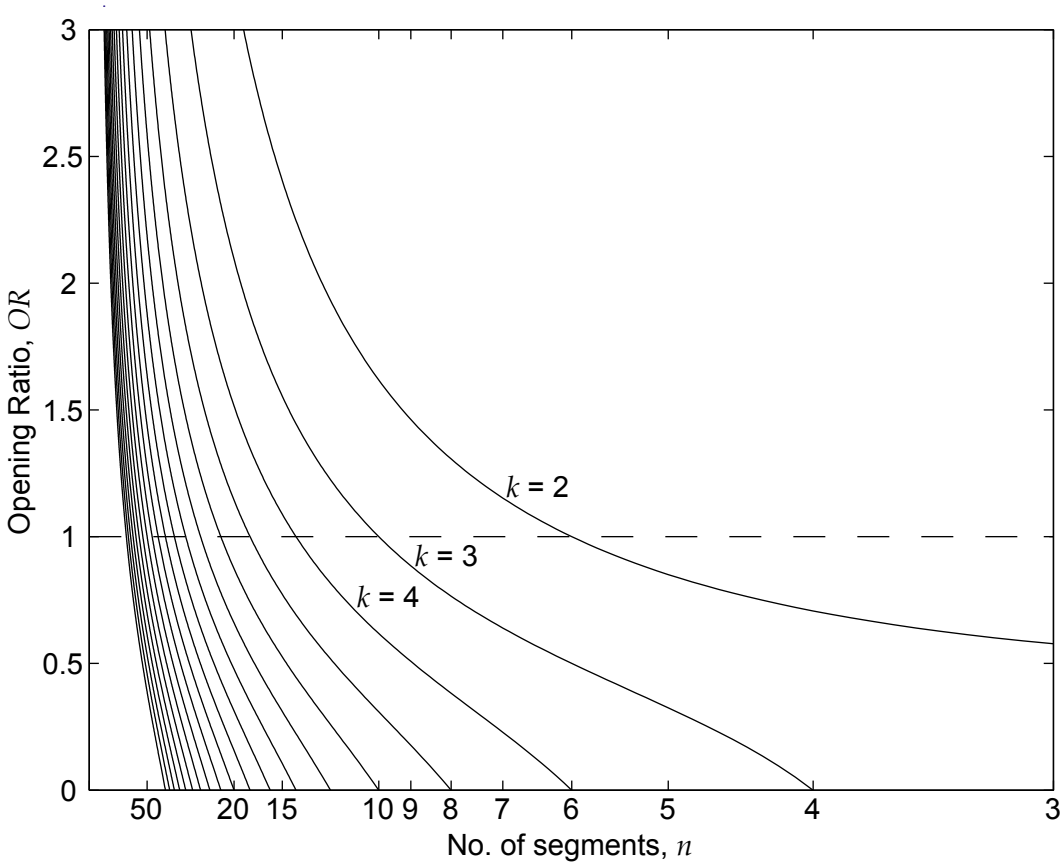

Figure 2.2: OR as a function of n and k

and is plotted for an arbitrary structure in Figure 2.3.

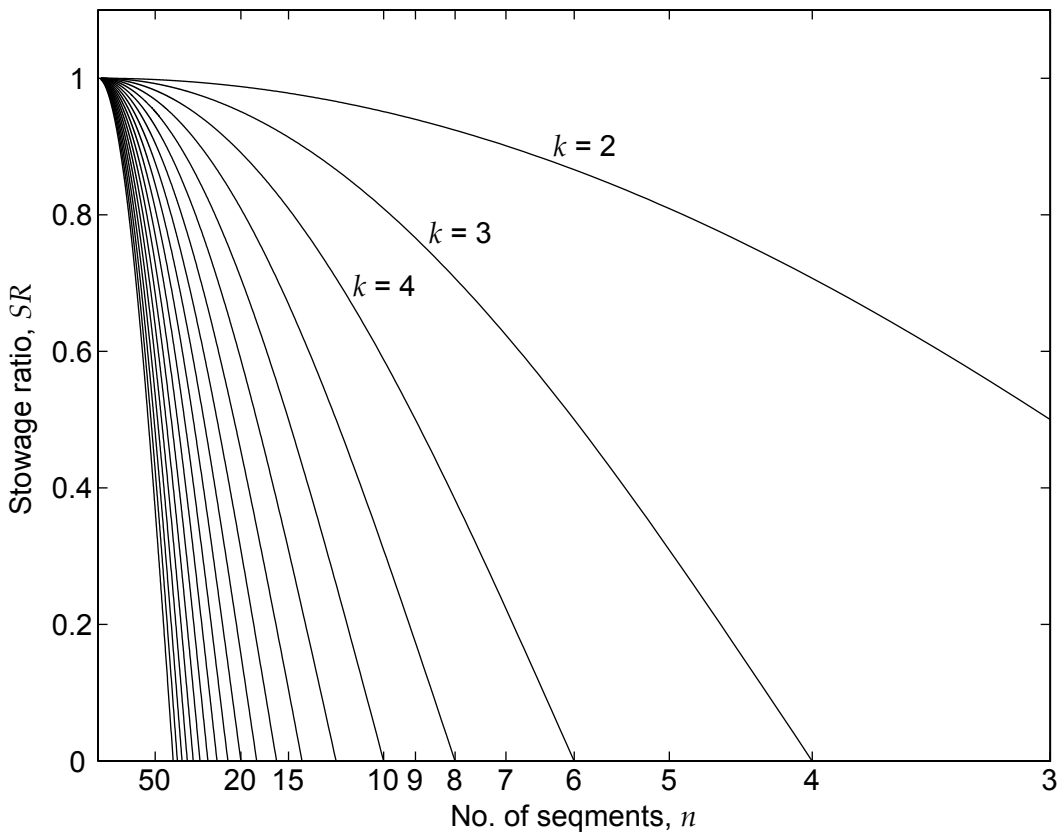

Figure 2.3: SR as a function of n and n

The modified stowage ratio, $SR^\star$ is gives by:

$$SR^\star = \frac{R_{\max}}{r_{\max}} \cos\left(\frac{\pi}{n}\right) = \frac{\cos\left(\frac{\pi}{n}\right)}{\cos\left((k-1)\,\frac{\pi}{n}\right)} \tag{2.6}$$

$SR^\star$ is plotted as function of n and k in Figure 2.4.

2.2 Element Rotation

The motion of a single layer of angulated elements can be described by n circles, as found by Kassabian [7]. Thus the motion of the structure is also a rotation of each of its elements about the centre of its corresponding circle. The *rotation angle*, ϕ, is the total rotation undergone by an angulated element during the motion of the structure from the fully closed to the fully-open position.

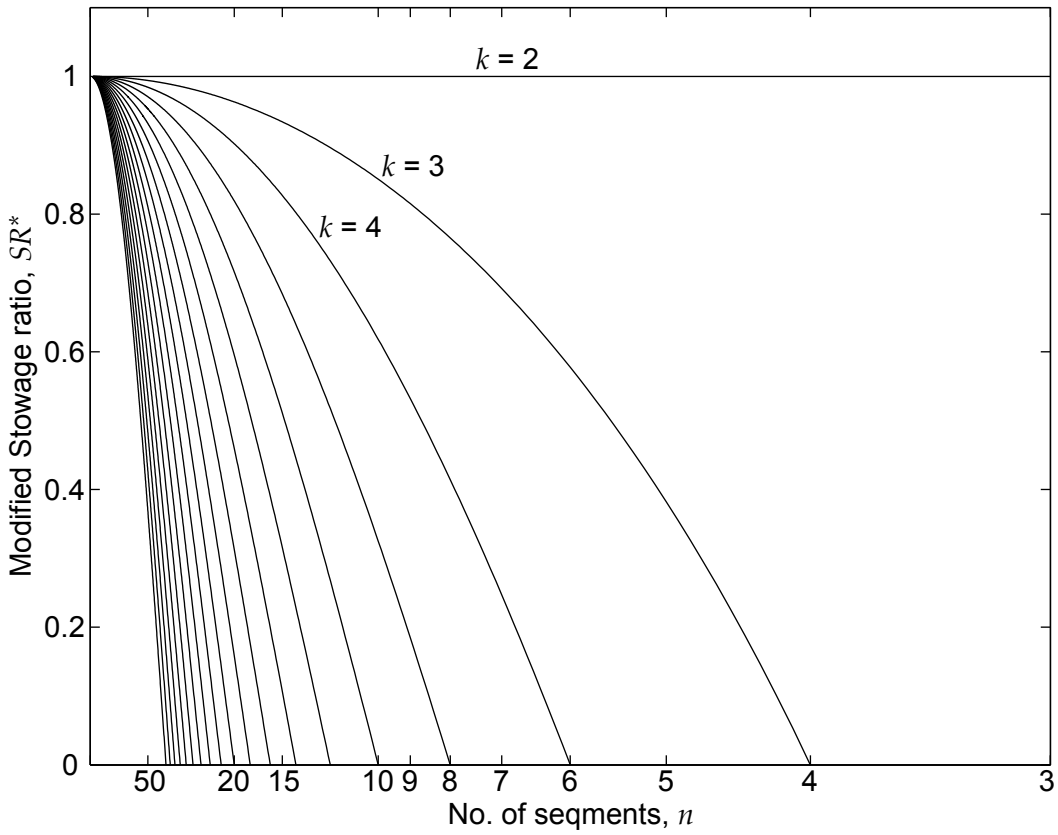

Figure 2.4: $SR^{\star}$ as a function of n and k

The rotation angle can be found by considering Figure 2.5 where the closed position is shown with all the angulated elements coinciding at the origin of the structure. Their circles of motion also intersect at the origin. The open position is reached when neighbouring angulated elements coincide at the point of intersection of their respective circles of motion. This corresponds to the point at which the outer rhombuses have been distorted so two diagonally opposite joints coincide and further motion is impossible.

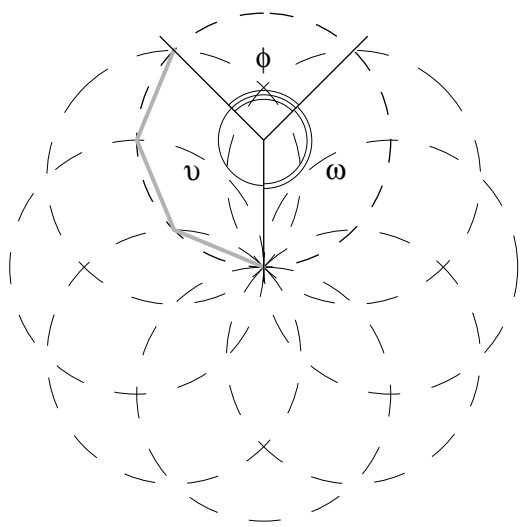

Figure 2.5: Angles υ, ϕ and ω on the circle of motion

The angle subtended by a single bar on the circle of motion is equal to:

$$\frac{2\pi}{n} = \alpha \tag{2.7}$$

Thus the *element angle*, subtended by the angulated element is obtained by multiplying α by the number of bars, k, that make up the angulated element:

$$\upsilon = k\frac{2\pi}{n} \tag{2.8}$$

The *limit angle*, subtended by the intersection points of two neighbouring circles of motion, corresponds to the two limits for the motion of the angulated element and is found from:

$$\omega = \pi - \frac{2\pi}{n} \tag{2.9}$$

The rotation angle can then be calculated from:

$$\phi = 2\pi - \omega - \upsilon = \pi + (1 - k)\,\frac{2\pi}{n} \tag{2.10}$$

This equation is plotted for variables k and n in Figure 2.6.

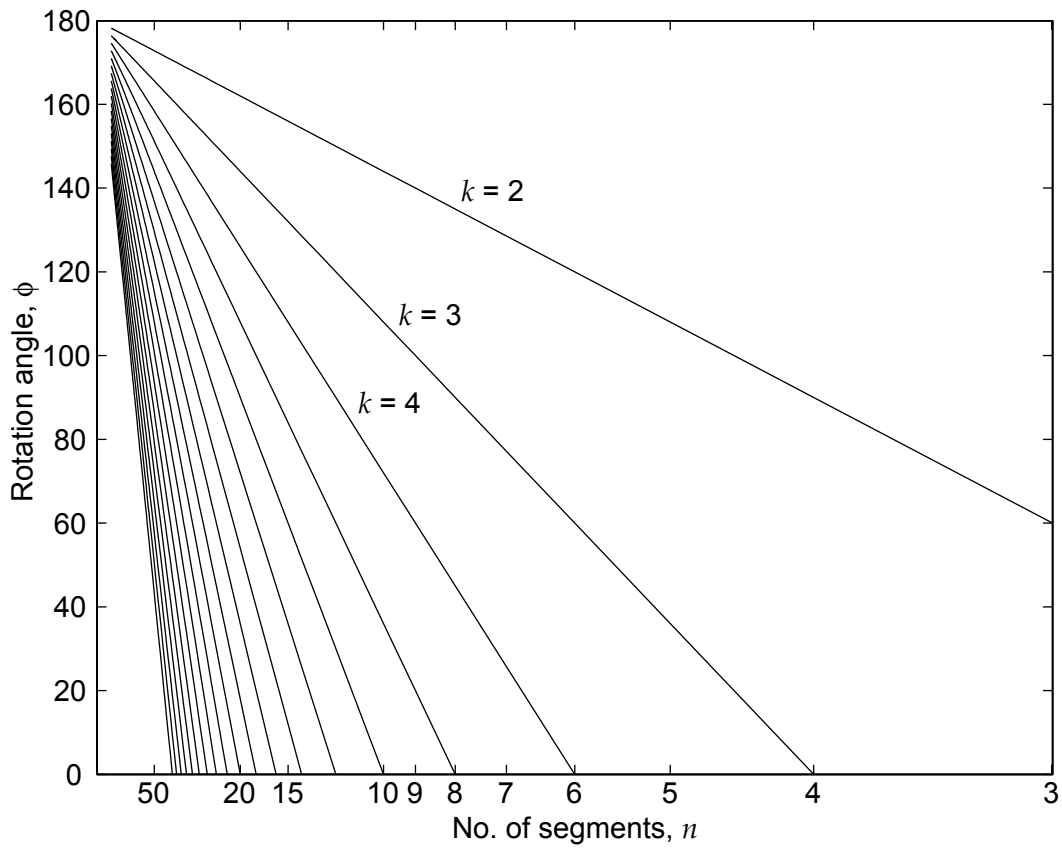

Figure 2.6: The angle of rotation, ϕ, as function of k and n

Figure 2.6 shows that for an increasing number of bars, k, per angulated element the rotation angle ϕ decreases and for an increase in the number of segments, n, with constant k the angle is increased.

Setting ϕ equal to *zero* the maximum number of bars for a given number of segments can be found from Equation 2.10:

$$0 \leq \phi = \pi + (1 - k)\,\frac{2\pi}{n} \Rightarrow k \leq \frac{n}{2} + 1 \tag{2.11}$$

2.3 Reduction Angles

As will be shown in Section 2.4 the bar structure will not always be able to reach the fully open and closed positions. This can be due to a number of reasons, such as elements or joints colliding before the extreme positions are reached. To include this effect the equations above must be modified and this is done by introducing the two *reduction angles*, ψ_1 and ψ_2. These denote the corrections needed respectively for the closed and open positions, as shown in Figure 2.7. The rotation angle is thus modified to:

$$2\pi = \omega + \phi^\star + \upsilon + \psi_1 + \psi_2 \tag{2.12}$$

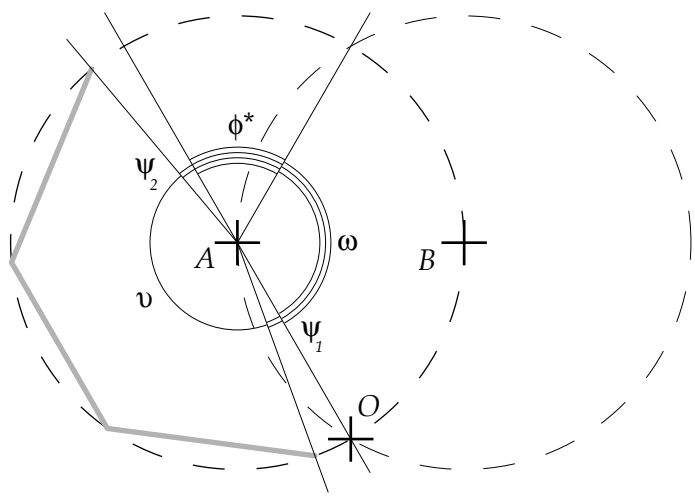

Figure 2.7: Definition of the reduction angles ψ_1 and ψ_2, in the closed position

The *reduced* rotation angle is a function of n, k, ψ_1 and ψ_2:

$$\phi^\star = \pi + (1-k)\,\frac{2\pi}{n} - \psi_1 - \psi_2 \tag{2.13}$$

It can be compared with Equation 2.10.

The radii defined in Section 2.1 are modified to accommodate the reduced rotation angle. From Figure 2.8 showing the circle of motion for one particular angulated element:

$$r_{\min} = 2r^\star \sin\left(\frac{\psi_1}{2}\right) \tag{2.14}$$

and

$$R_{\min} = 2r^{\star} \sin\left(\frac{\upsilon + \psi_1}{2}\right) \tag{2.15}$$

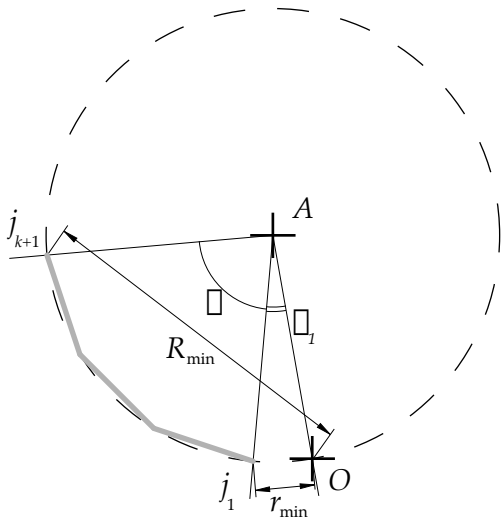

Figure 2.8: Dimensions for closed position

Similarly from Figure 2.9:

$$r_{\max} = 2r^{\star} \sin\left[\frac{1}{2}\left(\pi - (k-1)\,\alpha - \psi_2\right)\right] = 2r^{\star} \cos\left[(k-1)\,\frac{\pi}{n} + \frac{\psi_2}{2}\right] \tag{2.16}$$

and

$$R_{\max} = 2r^{\star} \sin\left(\frac{\pi - \psi_2}{2}\right) = 2r^{\star} \cos\left(\frac{\psi_2}{2}\right) \tag{2.17}$$

Equations 2.14 to 2.17 could be plotted, as in Section 2.1, for various values of the reduction angles.

2.4 Joint Size Effect

In practical structures all elements will have a finite size, which will limit the motion of the structure as the elements will interfere with each other.

In Section 2.2, it was shown that the bar structure can be considered to be made from *two* separate layers of angulated elements; these layers are inter-connected

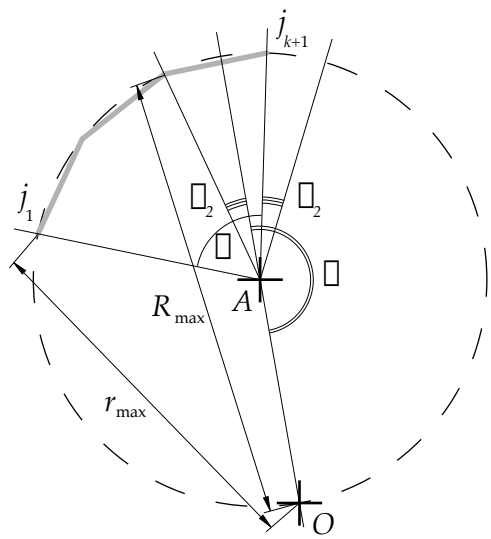

Figure 2.9: Dimensions for open position

by the joints of the structure. Of course an element in one layer cannot interfere with any element in the other layer. When considering contact between different elements, it is therefore possible to analyse only one layer of the structure. This is what will be done from now on in this report.

In the following analysis the joints are defined as circular and with radius r_j. The *joint size* is expressed in the dimensionless form $r_j/r^\star$.

The open and closed positions of a bar structure with joints of finite size are shown in Figures 2.10 and 2.11. For easier reference, the joints are numbered starting from the innermost joint, j_1, and ending with the outermost joint, j_{k+1}. From the figure it can be seen that in the closed position the innermost joints are in contact. Further closing of the structure is therefore inhibited by contact between joints j_1. The opening of the structure is limited by contact between joints j_{k-1} and j_{k+1} as the two diagonally positioned joints in the outer ring of rhombuses collide. These limits occur for all configurations.

In this case the two limits for the motion are defined by the contact between joints and so the corresponding reduction angles can be found by considering Figure 2.12. Drawing a polygon through the centres of the joints j_1 the distance between the centres of the joints is:

$$\overline{MN} = 2r_j \tag{2.18}$$

From this:

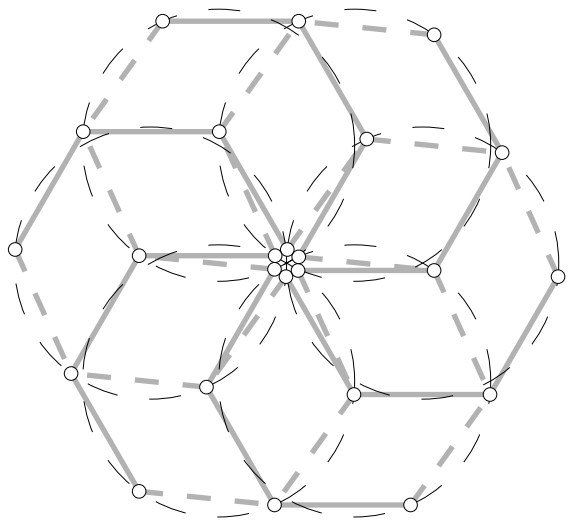

Figure 2.10: Closing limited by contact between joints j_1

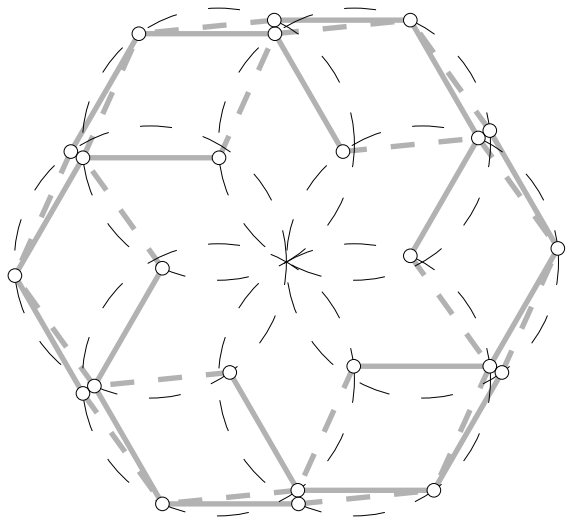

Figure 2.11: Opening limited by contact between joints j_{k-1} and j_{k+1}

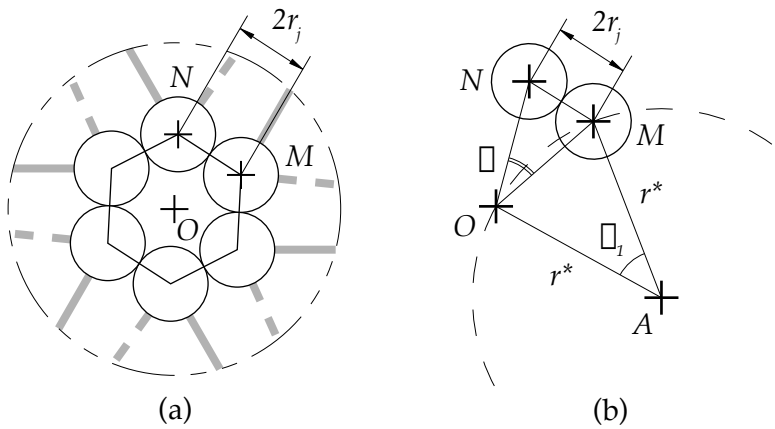

Figure 2.12: Determining the reduction angle ψ_1 (a) view of centre region (b) detail of two joints

$$\begin{aligned} \sin\left(\frac{\alpha}{2}\right) &= \frac{r_j}{\overline{OM}} \\ \overline{OM} &= \frac{r_j}{\sin\left(\frac{\pi}{n}\right)} \end{aligned} \tag{2.19}$$

As $\overline{OM} = r_{min}$, Equation 2.14 can be used to find the inner reduction angle:

$$\psi_1 = 2\arcsin\left(\frac{r_j}{r^\star}\frac{1}{2\sin\left(\frac{\pi}{n}\right)}\right) \tag{2.20}$$

A similar approach can be used to find ψ_2. It can also be shown that if joints j_1, j_{k-1} and j_{k+1} are of equal size then the reduction angles ψ_1 and ψ_2 are equal. If other joints in the structure are of *larger* size than r_j, then other limits might be imposed on the motion of the structure.

Equation 2.20 allows a simple design chart to be plotted. In Figure 2.13 the reduced rotation angle, $\phi^\star$, is found by subtracting the total reduction angle, $\psi_1 + \psi_2$, from the rotation angle, as shown in the figure. Similar design charts could be plotted for the ratios OR, SR and $SR^\star$, described in Section 2.1.

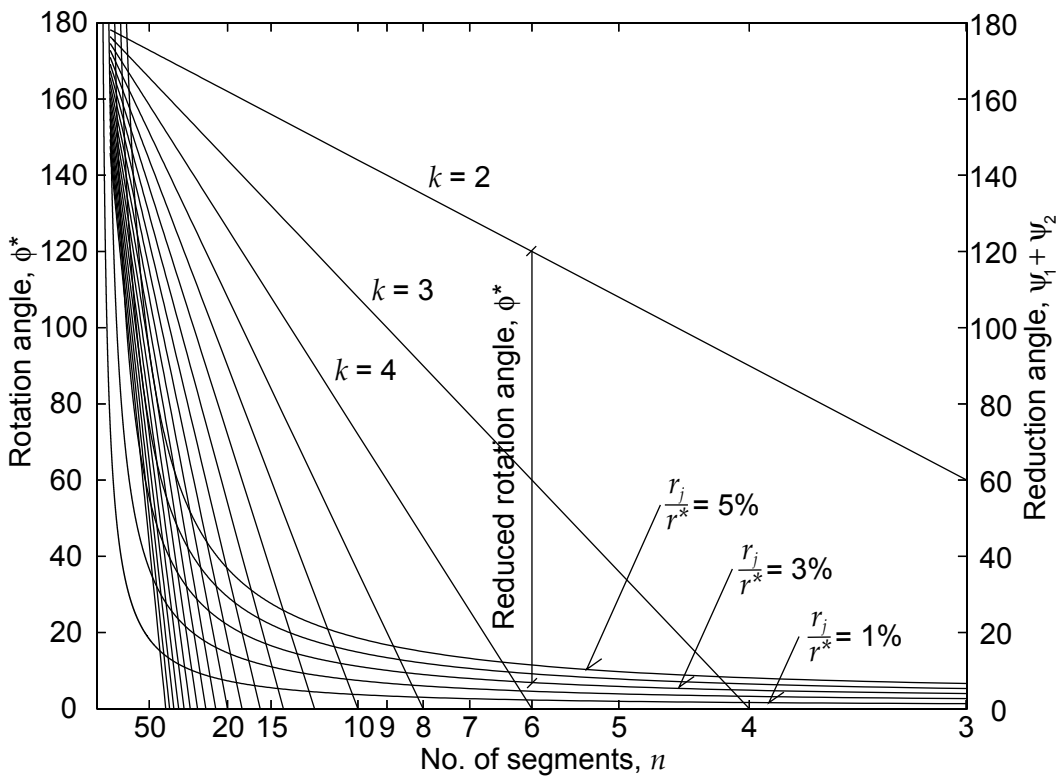

Figure 2.13: Determining the reduced rotation angle for various joint sizes

Chapter 3

Basic shape of Covering Plates

Two neighbouring angulated elements in the same layer are linked angulated elements in the other layer, thus form a series of rhombuses. In this chapter it is shown how to design rigid cover elements for the bar structureby considering how these rhombuses change shape when the angulated elements move. In fact, becourse a rhombus is a special case of a parallelogram, for generality parallelograms will be used in the following.

3.1 A Single Parallelogram

Consider a parallelogram made from the parallel bars a and b and a pair of parallel linking bars, as shown in Figure 3.1. Bar b is considered fixed so no rigid body motions are allowed and this leaves the structure with *one* mechanism which allows the linking bars to rotate and bar a to translate. The top-left angle defines the rotation angle, ϕ, as shown in Figure 3.1. This angle will later be shown to be equal to the rotation angle introduced in Section 2.2. All rotation angles are defined to be positive if clock-wise.

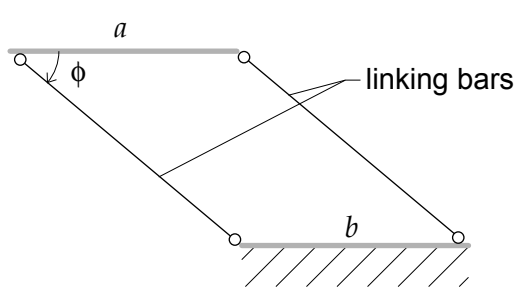

Figure 3.1: Parallelogram

3.1.1 Inclination angle

Consider a rigid plate attached to both bars a and b. This rigid body eliminates the mechanism of the parallelogram. If a straight cut at an *inclination angle* Λ is made in the plate then the structure will regain its mechanism. The line of the cut is called the *inclination line*. Because the two plates are not allowed to overlap, the angle ϕ can only increase, or decrease – depending on the inclination angle. In each case, the motion of the parallelogram has to stop when the gap between the two plates is closed again. This is shown in Figure 3.2.

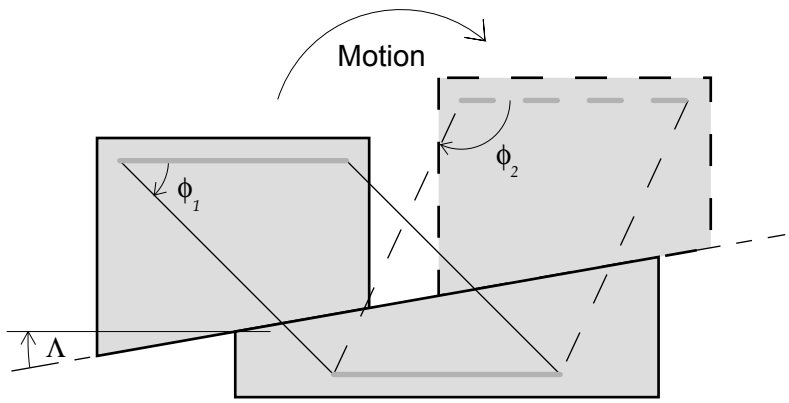

Figure 3.2: Motion of parallelogram with two rigid plates

The two limits on the rotation angle are denoted by ϕ_1 and ϕ_2, and knowing these Λ can be found. From Figure 3.3 the angle ξ is found:

$$\xi = \phi_1 + \Lambda \tag{3.1}$$

Considering the sum of angles for triangle ABC:

$$\pi = 2\xi + \phi_2 - \phi_1 \tag{3.2}$$

The inclination angle can thus be found:

$$\begin{aligned} \pi &= 2\Lambda + (\phi_2 + \phi_1) \\ \Lambda &= \frac{\pi - \phi_1 - \phi_2}{2} \end{aligned} \tag{3.3}$$

As no length variables are present in Equations 3.1 and 3.3, the position of the inclination line relative to the parallelogram has no influence on the limits for the angle of rotation.

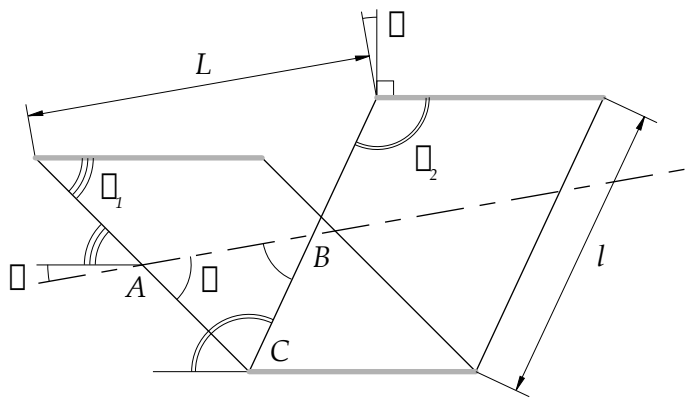

Figure 3.3: Angles and distance for a rotation in the parallelogram

For $\phi_1 = \pi - \phi_2$ the inclination line is found to be parallel to bars a and b:

$$\Lambda = \frac{\pi - \phi_1 - \phi_2}{2} = \frac{\pi - \pi + \phi_2 - \phi_2}{2} = 0 \tag{3.4}$$

For $\phi_2 = \pi$, bars a and b of the parallelogram have become colinear and:

$$\Lambda = \frac{\pi - \phi_1 - \phi_2}{2} = \frac{\pi - \phi_1 - \pi}{2} = -\frac{\phi_1}{2} \tag{3.5}$$

These solutions will be used below.

3.1.2 Shift along inclination line

Figure 3.3 shows how bar a moves a distance distance L, called shift, parallel to the inclination line during the motion. L can be found from:

$$L^2 = l^2 + l^2 - 2l^2 \cos(\phi_2 - \phi_1) = 2l^2 \left(1 - \cos(\phi_2 - \phi_1)\right) \tag{3.6}$$

Where l is the length of the linking bars.

As the shift is a function of the total angle of rotation and the length of the linking bars, both of which are known for the circular structure described in Chapter 2, it can be found readily.

3.2 Inter-connected Parallelograms

Two identical parallelograms A and B can be connected to each other so that they share a common linking bar. Hence the bars a_1 and a_2 form a single continuous angulated element and similarly for bars b_1 and b_2. These bars are connected with a kink of angle σ. The rotation angle for the two parallelograms has a difference of σ as the rotation angle in each parallelogram is measured relative to the respective linking bars, as shown in Figure 3.4. This can be written in the form:

$$\phi^B = \phi^A + \sigma \tag{3.7}$$

If two plates are attached to parallelograms A and B respectively two cuts must be made for the inter-connected parallelogram to regain its mechanism. If the limits for parallelogram A, ϕ_1^A and ϕ_2^A, are determined then the limits for parallelogram B, ϕ_1^B and ϕ_2^B, can be found from Equation 3.7.

The two inclination angles for the parallelograms:

$$\Lambda^A = \frac{\pi - \phi_1^A - \phi_2^A}{2} \tag{3.8}$$

and

$$\Lambda^B = \frac{\pi - \phi_1^B - \phi_2^B}{2} \tag{3.9}$$

However, by substituting Equation 3.7 into Equation 3.9 the inclination lines for the two parallelograms are found to be parallel:

$$\begin{aligned} \Lambda^B &= \frac{\pi - (\phi_1^A + \sigma) - (\phi_2^A + \sigma)}{2} \\ &= \frac{\pi - \phi_1^A - \phi_2^A}{2} - \sigma = \Lambda^A - \sigma \end{aligned} \tag{3.10}$$

Thus a single rigid plate can be attached to the inter-connected parallelograms and cut by a single line without the motion of either of the two parallelograms is restricted. As the inclination angles are equal for the parallelograms it can be determined by only considering a single parallelogram.

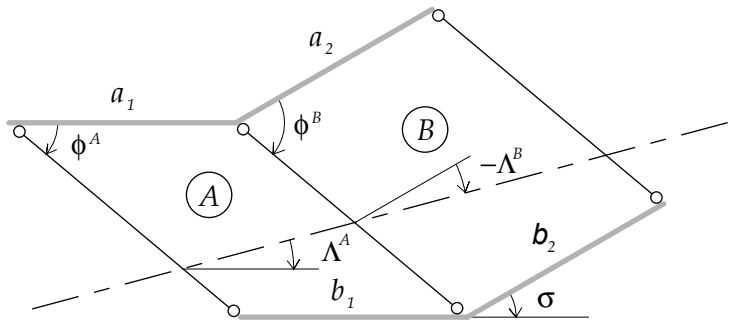

Figure 3.4: Two connected parallelograms

3.3 Multi-angulated parallelograms

For the bar structure the above results can be used to find the shape of cover elements which can be attached to the bar structure without restricting its motion.

Two neighbouring angulated elements in the same layer form, together with bars in the elements of the other layer, a series of rhombuses. The limits to the rotation of these rhombuses are determined by the overall configuration of the structure. It is therefore possible to define two plates, using a single inclination line, that can be attached to the angulated elements without restricting their motion.

Consider two neighbouring angulated elements in a structure with $k = 3$, as shown in Figure 3.5. The three-bar elements, a_1-a_3 and b_1-b_3, and the linking bars create two rhombuses, A and B. Rhombus A is created from the parallel bars a_1 and b_2 and B from a_2 and b_3. In the closed position the bars a_1 and b_1 subtend an angle α as the left-hand-side ends of the angulated elements coincide at the origin O of the bar structure, thus giving:

$$\phi_1^A = \alpha \tag{3.11}$$

These bars are connected with kink angles $\sigma = \alpha$ as shown in Figure 1.14. From Equation 3.7:

$$\phi_1^B = \phi_1^A + \sigma = 2\alpha \tag{3.12}$$

The limit for the open position is found by noting that bars a_2 and b_3 of rhombus B become colinear when $\phi_2^B = \pi$, as illustrated in Figure 3.5 (b).

$$\phi_2^B = \pi \tag{3.13}$$

And following Equation 3.7:

$$\phi_2^A = \phi_2^B - \sigma = \pi - \alpha \tag{3.14}$$

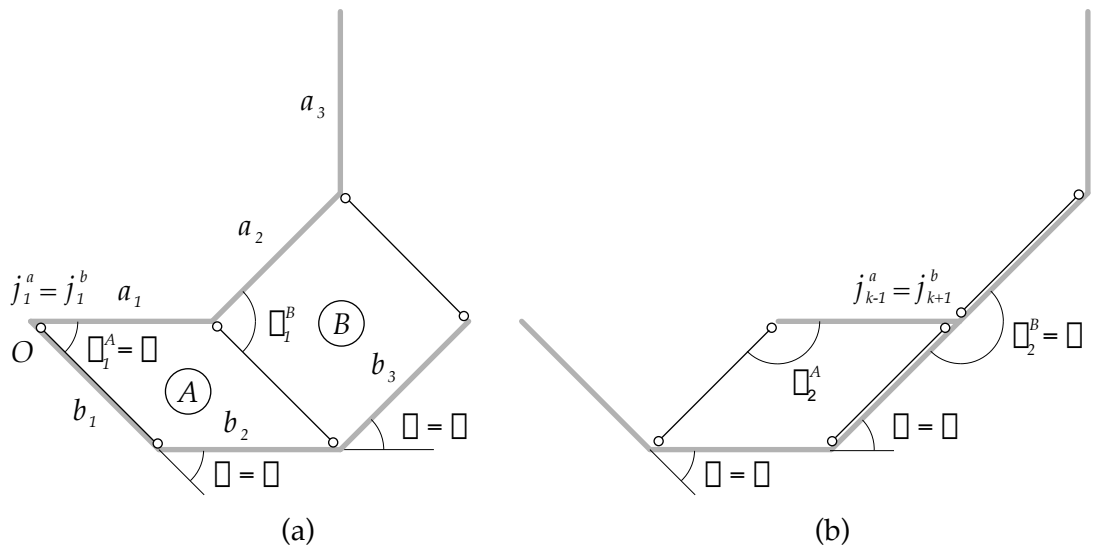

Figure 3.5: The two limit positions for neighbouring angulated elements.

These solutions were already considered in Section 3.1.1 giving:

$$\phi_1^A = \pi - \phi_2^A \Rightarrow \Lambda^A = 0 \tag{3.15}$$

and:

$$\phi_2^B = \pi \Rightarrow \Lambda^B = -\frac{\phi_1^B}{2} = -\alpha \tag{3.16}$$

This verifies Equation 3.10 as:

$$\Lambda^B = \Lambda^A + \sigma \Rightarrow -\alpha = -\alpha \tag{3.17}$$

As the inclination line can be drawn at any position, as long it is at the correct inclination angle, a criterion for the absolute position is needed.

Considering the complete bar structure, a series of inclination lines can be drawn between the angulated elements. This creates n wedge shaped cover elements, each subtending an angle α.

The tips of these cover elements must coincide at the centre of the structure to avoid gaps. Thus in Figure 3.5 the inclination line has to pass through joint j_1 of the angulated elements. The inclination line also passes trough the outer joint of the angulated element b, j_{k+1}, and node j_{k-1} for element a.

Later on, it will prove useful to define the inclination line in relation to element b rather than a, thus the angular difference α is added to Equation 3.3:

$$\Lambda = \frac{\pi - \phi_1 - \phi_2}{2} + \alpha \tag{3.18}$$

To define the cover elements it is therefore only necessary to define a single inclination line as both boundaries of the element are defined when similar inclination lines are defined for all angulated elements. Figure 3.6 shows the wedge shaped cover elements created by the inclination lines for a structure with the configuration 8;3.

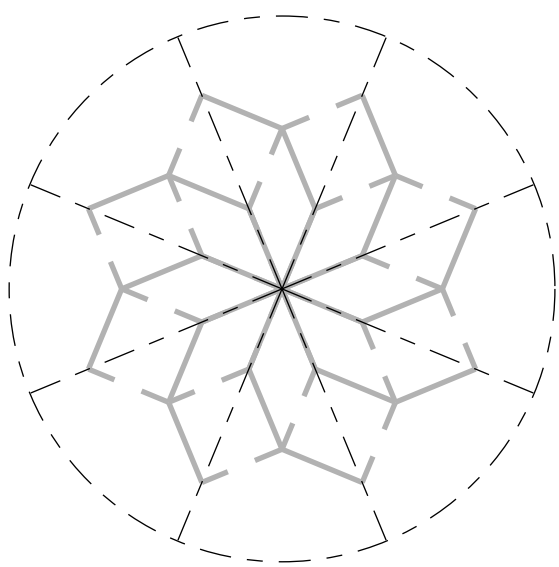

Figure 3.6: Wedge shaped plates created by the inclination lines

If a configuration n;k is considered, the two angulated elements will be linked so that k - 1 rhombuses are created. Following the approach above, the first rhombus, A, and the last, Z, will determine the limits for all rhombuses.

For A Equation 3.11 is unchanged and for Z the limit angle in the closed position is derived as it was for B, by use of Equation 3.7:

$$\phi_1^Z = (k-1)\alpha \tag{3.19}$$

For the open position we have from Equation 3.13:

$$\phi_2^Z = \pi \tag{3.20}$$

And using Equation 3.7 the limit angle for A is found:

$$\phi_2^A = \pi - (k-2)\alpha \tag{3.21}$$

Only a single rhombus needs to be considered for determining the inclination angle using Equation 3.18.

As explained in Section 2.2 there is a maximum limit for k for a given number of segments n. This limit is found again from $\pi \geq \phi_1^Z$ thus verifying Equation 2.11:

$$\begin{aligned} \pi &\geq \phi_1^Z = (k-1)\alpha \\ k &\leq \frac{n}{2} + 1 \end{aligned} \tag{3.22}$$

3.4 Rotation angles

The rotation angles for the rhombuses and the angulated elements can be found to be equal by rearranging Equation 2.10 using Equation 1.1:

$$\phi = \pi - (k-1)\alpha \tag{3.23}$$

Rearranging Equation 3.21 and inserting ϕ from Equation 3.23:

$$\phi_2^A = \pi - (k-1)\alpha + \alpha = \phi + \alpha \tag{3.24}$$

From Equation 3.11 we have $\phi_1^A = \alpha$ and thus the rotation in the rhombus is:

$$\phi_2^A - \phi_1^A = \phi + \alpha - \alpha = \phi \tag{3.25}$$

The rotation in the rhombuses is therefore equal to that of the angulated elements. Using the same approach $\phi^\star$ can also be found to be equal and therefore Equation 3.6 can be simplified:

$$\begin{aligned} L^2 &= 2l^2 - 2l^2 \cos\phi^\star \\ L &= l\sqrt{2 - 2\cos\phi^\star} \end{aligned} \tag{3.26}$$

To simplify the method for finding the inclination angle, Equation 3.25 is substituted into Equation 3.18 and re-arranged:

$$\Lambda^A = \frac{\pi - \phi - 2\phi_1^A}{2} + \alpha \tag{3.27}$$

Using Equations 1.1, 3.11 and 3.23:

$$\Lambda^A = \frac{\pi - (\pi + (1-k)\alpha) - 2\alpha + 2\alpha}{2} = \frac{(k-1)\alpha}{2} = (k-1)\frac{\pi}{n} \tag{3.28}$$

This equation confirms that wedge shaped cover elements, defined with their tip coinciding with the origin of the structure and their boundaries passing through the outer joints of the angulated elements, will not have gaps or overlaps in the surface, neither in the open nor in the closed position. This was also found by Kassabian [7].

3.5 Reduction angles

In Section 2.3 reduction angles were introduced to account for practical limits in the motion of the structure and these led to the derivation of the reduced rotation angle. The reduction angles are included in the definition of the inclination angle by modifying the limits for the parallelograms:

$$\phi_1^\star = \phi_1^A + \psi_1 \tag{3.29}$$

And

$$\phi_2^\star = \phi_2^A - \psi_2 \tag{3.30}$$

Substituting Equations 2.13 and 3.29 into Equation 3.27 the following *reduced* inclination angle is obtained:

$$\Lambda^\star = (k-1)\frac{\pi}{n} - \frac{\psi_1}{2} + \frac{\psi_2}{2} \tag{3.31}$$

From this equation it can be seen that if the two reduction angles are equal, then the solution is a line parallel to that of the original solution in Equation 3.28.

3.5.1 Position of cover elements

In Section 3.3 the cover elements were defined with their tips always coinciding with the origin of the structure in the closed position. However it is possible to have alternative arrangements.

Without restricting the motion of the structure the position of the cover elements can be varied along radial lines. The radial position of the tip is expressed by the two components t and s as it will later prove helpful to use these components rather than a single radial coordinate. t is perpendicular to the inclination line and s is parallel to the line. This still produces a gap free, continuous cover for the structure. However, an opening with the diameter t and the shape of a n–sided polygon results at the centre of the structure in the closed position, see Figure 3.7. The relationship between t and s:

$$s = t \tan \frac{\alpha}{2} \tag{3.32}$$

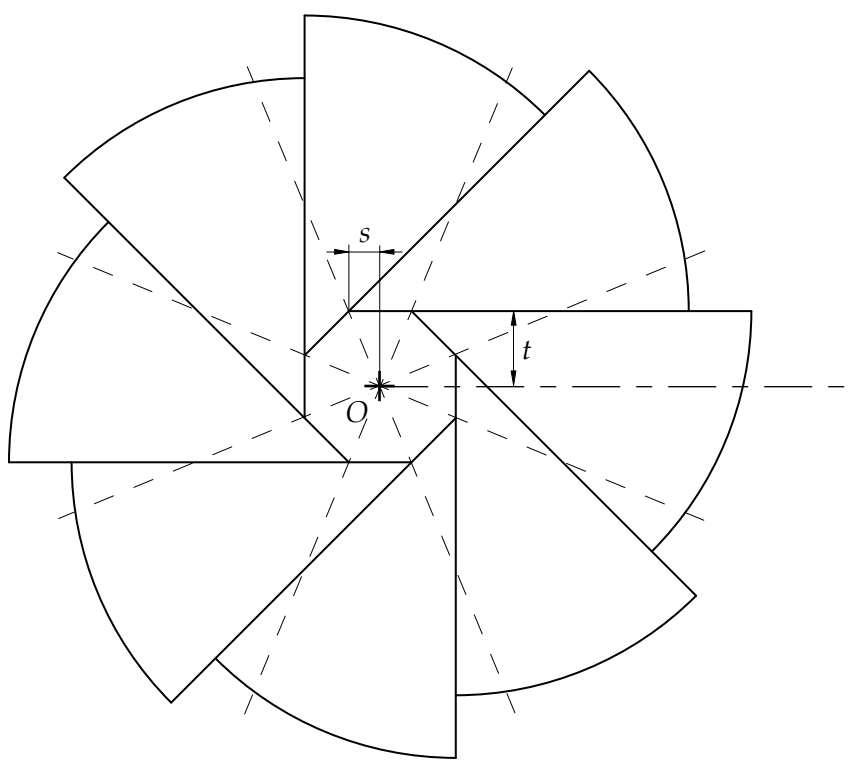

Figure 3.7: Wedge plates moved by the distances t and s

Chapter 4

Modified Shapes

Further work on the properties of parallelograms shows it is possible to make some changes to the wedge shaped cover elements that were derived in the previous chapter. All of the modified shapes that will be proposed exploits a periodicity in the motion of interconnected parallelograms. This chapter describes a method for finding this periodicity and it is applied for permutating the shape of the cover elements.

4.1 Further properties of parallelograms

During the motion of the parallelogram in Figure 3.3, bar a shifts by L relative to bar b, as found in Section 3.1.2. In fact, a whole cover element shifts by this amount, as shown in Figure 4.1. The shift is parallel to the inclination line and therefore a point on the boundary of one cover element will come into contact with two different points y on the other element, in the two extreme positions, see Figure 4.1. The distance between the two points of contact is the shift L.

Consider two cover elements a and b, which have a *non*-straight boundary as shown in Figure 4.1. The shared boundary between the two elements is shifted as the parallelogram is distorted. Therefore the edge of plate b must have the same features at two different positions to prevent overlap and gaps between the plates. If the common boundary between the two elements is longer than L, then the same features of b must be repeated also in a. Hence, cover elements with common boundaries longer than L must be such that all features have a periodic pattern as shown in Fig 4.2. As the motion is parallel to the straight inclination line, the periodicity of the boundary is expressed in terms of a distance parallel to the inclination line.

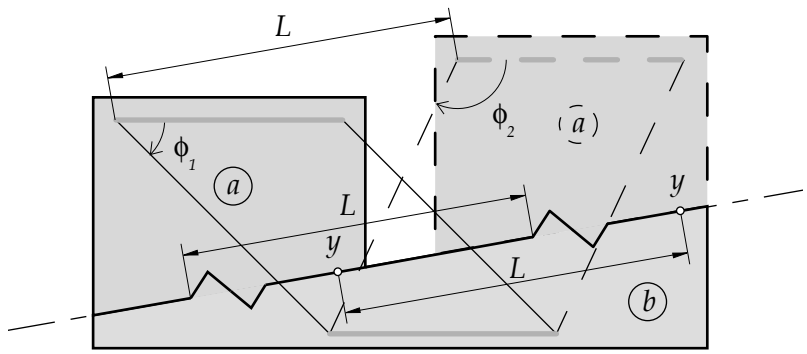

Figure 4.1: Point y shifts by a distance L during motion

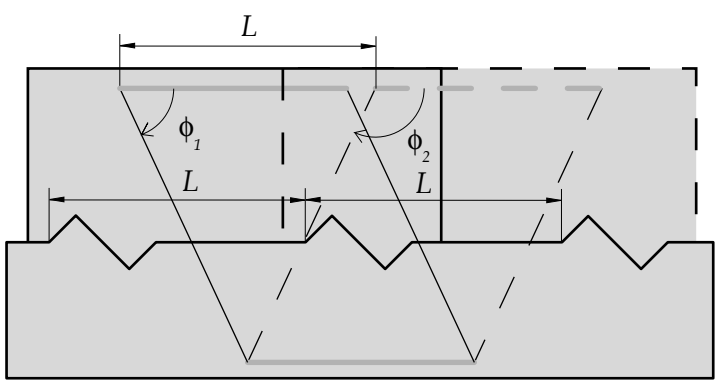

Figure 4.2: Plates with period L

4.2 Limits on Modified Shapes

Not all modified shapes that satisfy the rule of periodicity are possible. The velocity of any point on a cover element is instantaneously perpendicular to the linking bars, and equal to the velocity of the bar that it is attached to. Thus, by describing the instantaneous velocity of a joint in the parallelogram, the motion of all other points is also found. This can be used to describe the limits for shape changes of the cover elements that do not inhibit the motion.

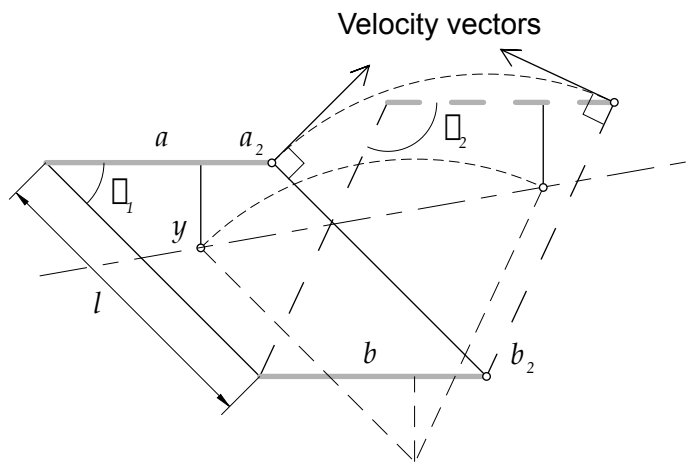

Figure 4.3: Motion of bar a in parallelogram and attached point y

Figure 4.3 shows the motion of a parallelogram and the path of joint a_2 on bar a. It can be seen that the motion of a_2 is circular, with a radius equal to the length of the linking bars, l. The centre of rotation is at the opposite end of the linking bar. The velocity vector for a_2 is shown in the figure. Point y, attached to bar a, has identical velocity.

The direction of the velocity vector can be related to the inclination line using Figure 4.4:

$$\Delta = \Lambda + \phi - \frac{\pi}{2} \tag{4.1}$$

The tangent to the boundary of the cover elements must be within the bounds of Δ_{max} and Δ_{min} as motion is otherwise inhibited. These bounds are found by considering the directions of the velocity vectors at the extreme positions ϕ_1 and ϕ_2.

The circular arc that describes the motion of a point on the boundary of element a will limit the extent to which element b can extend. This imposes a limit on the shape changes that are possible. The maximum distance, h, from the inclination

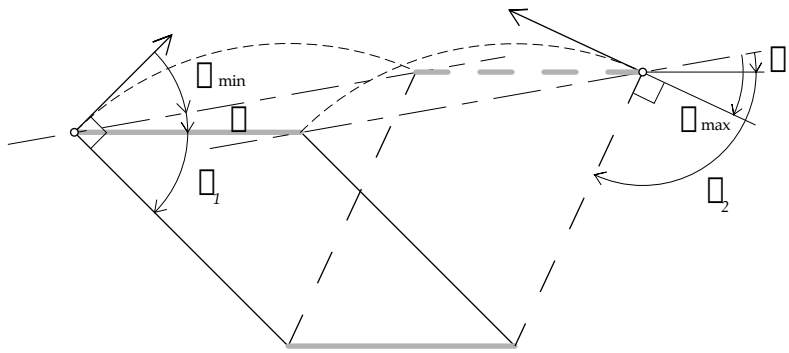

Figure 4.4: Direction of velocity vector in the two extreme positions

line to the boundary can therefore be found from Figure 4.5:

$$h = l\left(1 - \sqrt{1 - \left(\frac{L}{2l}\right)^2}\right) \tag{4.2}$$

Using Equation 3.26:

$$h = l\left(1 - \sqrt{\frac{1}{2} + \frac{1}{2}\cos\phi^\star}\right) \tag{4.3}$$

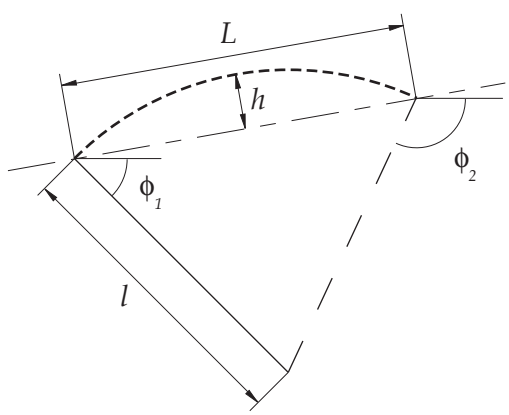

Figure 4.5: The maximum deviation h from the straight inclination line

The same limit applies to the boundary of element b. This is found by fixing bar a and letting bar b rotate with its attached element. Limits for both elements are shown in Figure 4.6 with the limits repeated periodically along the inclination line.

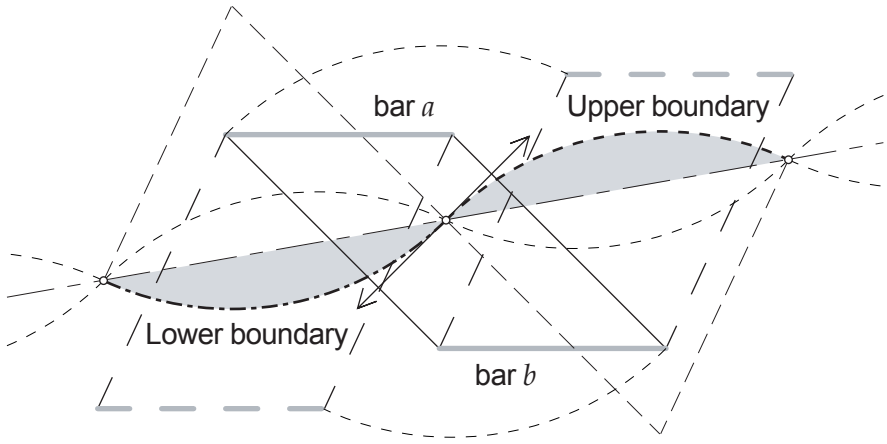

Figure 4.6: Upper and lower boundaries established through the motion of bars a and b respectively

Thus by defining a single point on the inclination line the limits for all possible shape changes can be determined. These limits are shown diagrammatically in Figure 4.7.

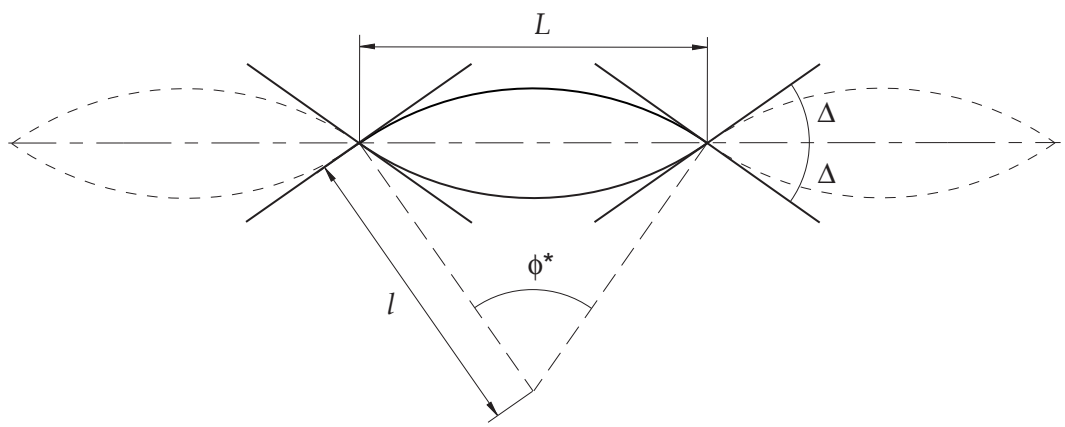

Figure 4.7: Design template for permutation of boundaries

4.3 Other shape considerations

The inclination lines define the overall shape of two sides of wedge shaped cover elements, but there is no kinematical requirement for the third side, along the perimeter of the structure. This is illustrated in Figure 4.8 which also demonstrates the shift along the boundaries.

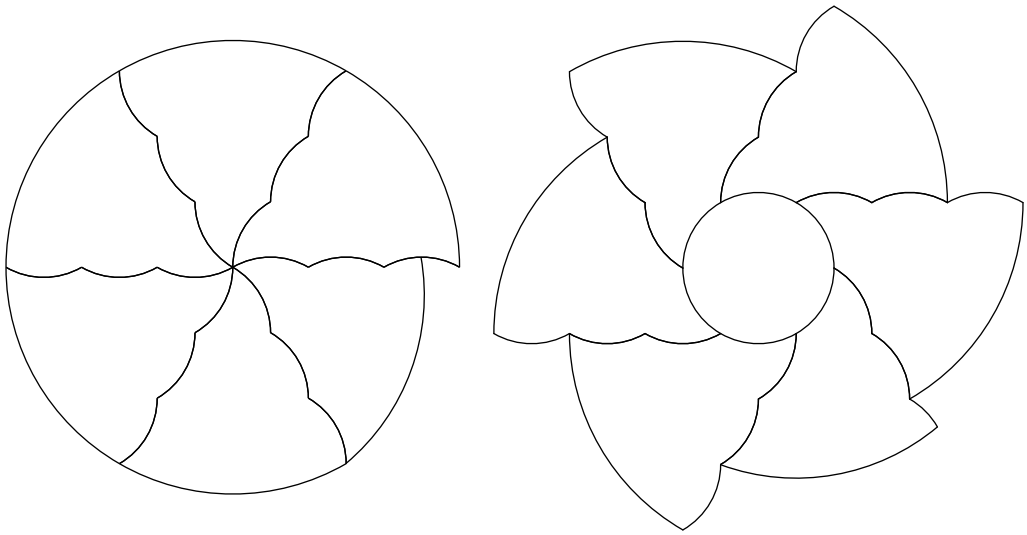

Figure 4.8: Demonstration of shift and boundary shapes for cover elements

4.3.1 Closing Central Gap

In Section 3.5.1 it was found that it is possible to vary the position of the cover elements so that an opening is created at the centre of the structure, in the closed configuration. In Figure 3.7 it can be seen that the initial part of the element boundary is not in contact with another element but with the central opening. This leaves the possibility of changing the shape of the boundary in this region, as the periodicity rule can be broken, as the shift is away from this part of the boundary. Because this part of the boundary will never be in contact with another element, non-periodic shape changes are therefore allowed.

Considering the velocity vectors of the tips of the cover elements, as shown in Figure 4.9, it is possible to determine the limits for shape changes in the central region. These shape changes can be used to determine the shape of a suitable cover for the central opening.

The key requirement is that the relative velocity of two neighbouring tip points, which is perpendicular to the average direction of the two as shown in Figure 4.10, must not be restricted. Therefore it is not possible to cover the complete central opening by extending less than *three* cover elements. See Figure 4.11 for two solutions.

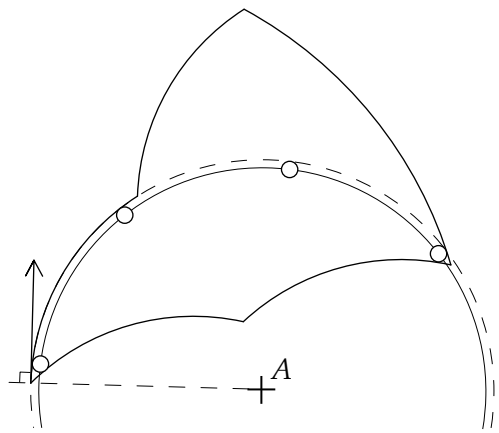

Figure 4.9: The velocity of the tip of the cover element

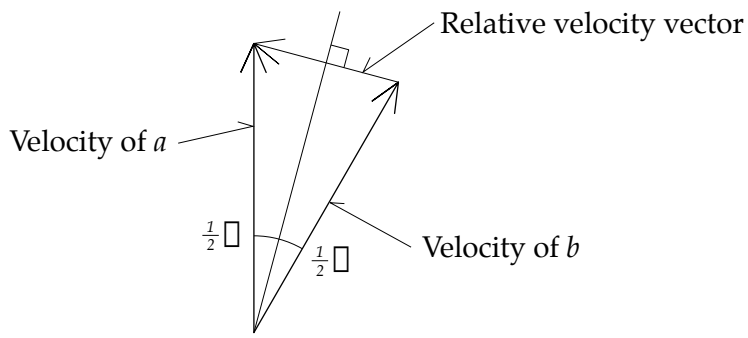

Figure 4.10: The relative motion between two neighbouring elements

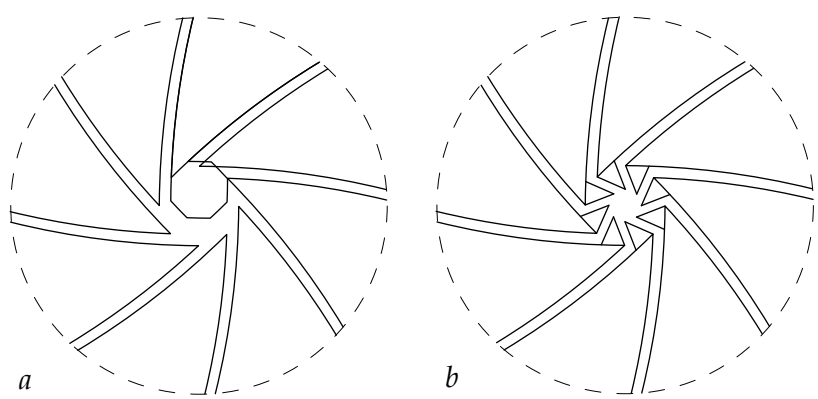

Figure 4.11: Solution a restricts the motion whereas b does not

Chapter 5

Design of Structures

Having defined the limits within which the shape of the cover elements can be varied, it is possible to design various structures using a unified approach.

In the following two different types of structures will be considered. The first is a bar structure which is covered by a layer of plate elements. It would be possible to use two layers of cover elements fixed to different layers of bars. As the motion of the structure is determined by the bar structure, the cover elements do not control or restrict the kinematics of the structure and thus each cover element can be fixed to an angulated bar element in many different ways.

The second type of structure is purely a plate structure and all the joints are directly between plate elements. This structure is made from two layers of identical plate elements that are designed so that the mechanism of this structure is equal to that of the previous bar structure.

The shapes described below are those for the structure in the closed position unless otherwise stated.

5.1 Bar Structure Covered by Plates

5.1.1 Covers with straight boundaries

For this type of structure the inclination lines always meet at the origin, hence there is no opening at the centre in the closed position, see Section 3.5.1. The shape of the individual elements is that of a wedge with two boundaries formed by the inclination lines. The third boundary and the extent of the cover element can be decided from criteria such as the visual appearance of the structure and the ratio between the dimension of the central opening and the extent of the outer boundary. This ratio is not necessarily equal to that described in Chapter 2,

which only dealt with the position of the bar structure.

The position of the inclination line is given by $t = 0$ and the inclination angle Λ is determined by the bar structure, using Equation 3.31. To cover the bar structure completely the cover elements need to have a minimum extent of R_{min}, Equation 2.15, if an overall circular shape is used. See Figure 3.6 for an example of such a design.

The design variables that govern the design of this type of structure are: The pair $n; k$ and the limit angles which will typically be determined by the joint size using Equation 2.20. The relative performance of the structure can be found from the design charts given in Chapter 2.

Note that generally a single cover element of this type will not completely cover the angulated element beneath it.

5.1.2 Covers with non-straight boundaries

As described in Chapter 4, it is possible to have non-straight boundaries for the cover elements. The covers will still preserve their basic wedge shape and all features must be (i) periodic and (ii) lie within the limits found in Section 4.2. The design in Figure 4.7 can be found for any structure using Equations 1.2, 2.13, 3.26 and 4.1.

Hence, it is possible to find particular designs of cover elements that achieve one or more design aims. One such aim is forming a circular central opening in the structure, in the open position.

5.1.3 Circular opening

To form a circular opening in the open position, the boundary of the cover elements must be formed by circular arcs. For the arcs to form a circle they must also join up at the ends in this position. Therefore the length of the arcs along the inclination line must be equal to the period L and the radius of the arcs must be equal to the radius of the opening, r_{max}. These conditions are satisfied by the design shown in Figure 4.8.

The smallest radius allowed within the limits for the boundary is $r = l$ and the largest is a straight line, $r \to \infty$. From this it is possible to write conditions for which it is possible to create a circular opening:

$$l \leq r_{max} \leq \infty \tag{5.1}$$

As the opening radius never reaches infinity this limit is omitted in the following.

From Equations 1.2 and 2.16 this becomes:

$$\begin{aligned} 2r^\star \sin\left(\frac{\pi}{n}\right) &\leq 2r^\star \cos\left[(k-1)\frac{\pi}{n} + \frac{\psi_2}{2}\right] \\ \frac{\pi}{n} &\leq \frac{\pi}{2} - (k-1)\frac{\pi}{n} - \frac{\psi_2}{2} \\ \psi_2 &\leq \pi - k\frac{2\pi}{n} \leq \pi - k\alpha \end{aligned} \tag{5.2}$$

For $\psi_2 = 0$ this can be reduced to a criterion for which configurations of bar structures with *zero*-sized joints will form circular openings if the radius of the arcs is r_{max}:

$$k \leq \frac{n}{2} \tag{5.3}$$

Considering Figure 5.1 the radius of the central opening can be redefined so that the radius is no longer defined by the position of joint j_1 but instead the tip of the wedge shaped cover element. The total reduction angle is defined:

$$\psi_{tot} = \psi_1 + \psi_2 \tag{5.4}$$

Using the total reduction angle Equation 2.16 is modified:

$$r_{\max} = 2r^\star \cos\left[(k-1)\frac{\pi}{n} + \frac{\psi_1}{2} + \frac{\psi_2}{2}\right] = 2r^\star \cos\left[(k-1)\frac{\pi}{n} + \frac{\psi_{tot}}{2}\right] \tag{5.5}$$

Also Equation 5.2 can then be re-written:

$$\psi_{tot} \leq \pi - k\frac{2\pi}{n} \tag{5.6}$$

Hence, if this requirement is satisfied then it is possible to design a structure that have an opening with a circular shape. However ψ_{tot} can also be substituted into Equation 3.31:

$$\Lambda^\star = (k-1)\frac{\pi}{n} - \psi_1 + \frac{\psi_{tot}}{2} \tag{5.7}$$

This result provides a very useful design tool and is shown in Figures 5.2 and 5.3. From the figure it can be seen that the position of the inclination lines is, for a constant ψ_{tot}, not influenced by changes of the values for ψ_1 and ψ_2. When ψ_1 is changed the angulated element is rotated by an equal amount in relation to the overall structure. The position of the inclination line will therefore remain constant in relation to the overall structure as ψ_1 is varied.

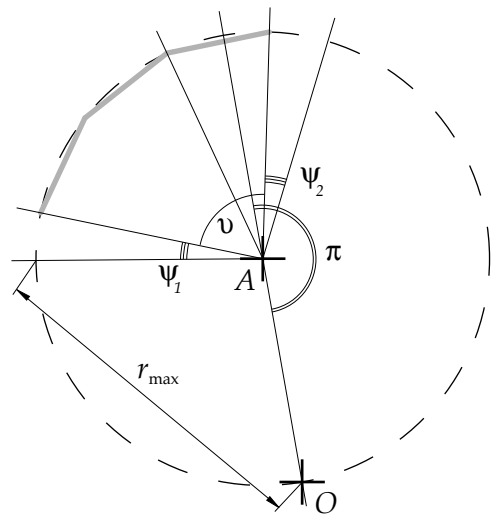

Figure 5.1: The radius of the opening when considering the tip of the cover

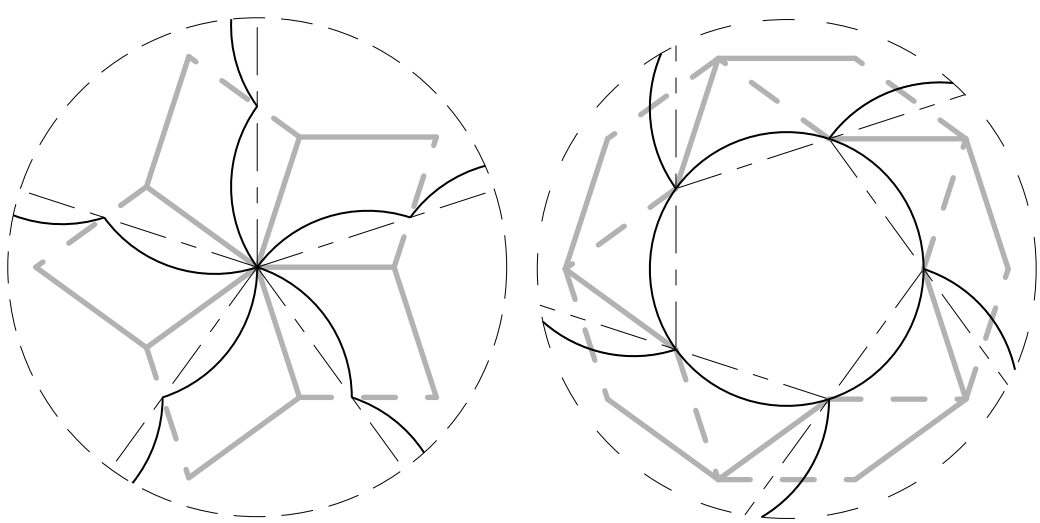

Figure 5.2: Cover elements with $\psi_1 = 0$ and $\psi_2 = 36°$

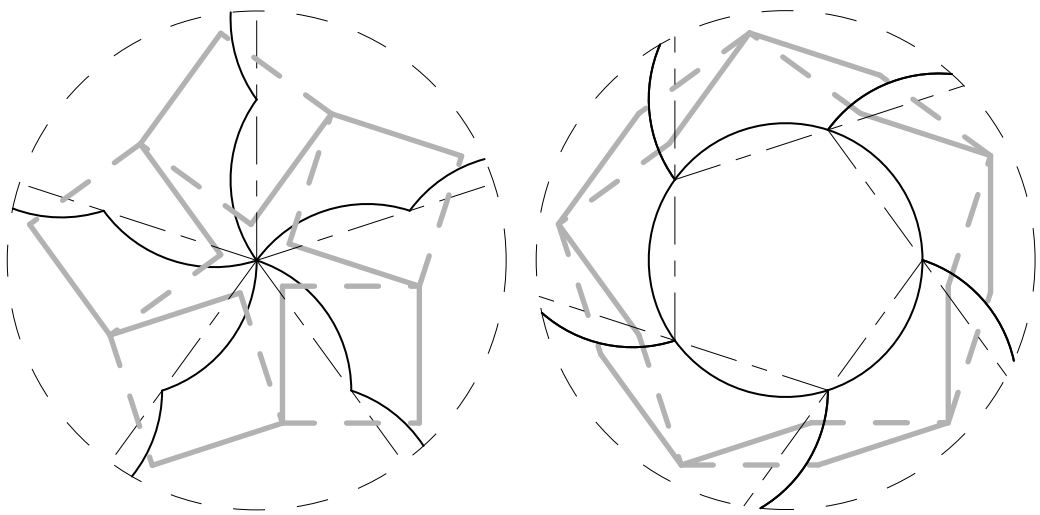

Figure 5.3: Cover elements with $\psi_1 = 18°$ and $\psi_2 = 18°$

5.1.4 Non-matching bar and plate structure

From Figure 5.4 it is seen that several configurations with different n;k have the same *non-reduced* rotation angle. These are found by drawing a horizontal line in the diagram; all intersections of this line with the lines obtained by plotting Equation 2.10 correspond to configurations with equal rotation angles.

This gives the possibility of designing structures with different numbers of angulated elements and cover elements. However, because each cover element can only be fixed to one angulated element, there must be at least as many angulated elements as covers. This principle is illustrated in Figure 5.5.

5.2 Plate Structures

In a plate structure that does not rely on a separate supporting bar structure, all joints must necessarily be present and connected in the same way as for the bar structure. This is the main design criterion for these plate structures.

For easier visualisation of the node positions, reference will still be made to the shape of the bar structure though this is no longer physically present. The plate elements can be divided into two groups: Straight boundaries and non-straight boundaries.

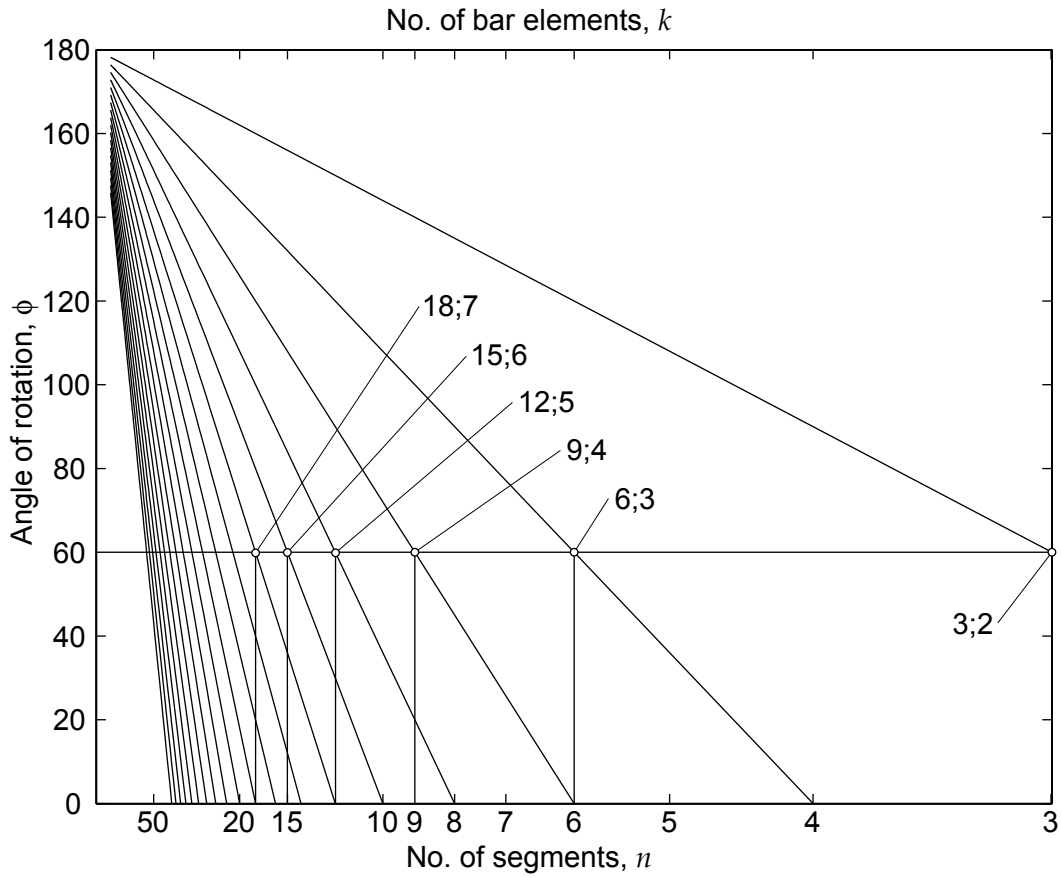

Figure 5.4: Configurations of $n;k$ with $\phi = 60°$

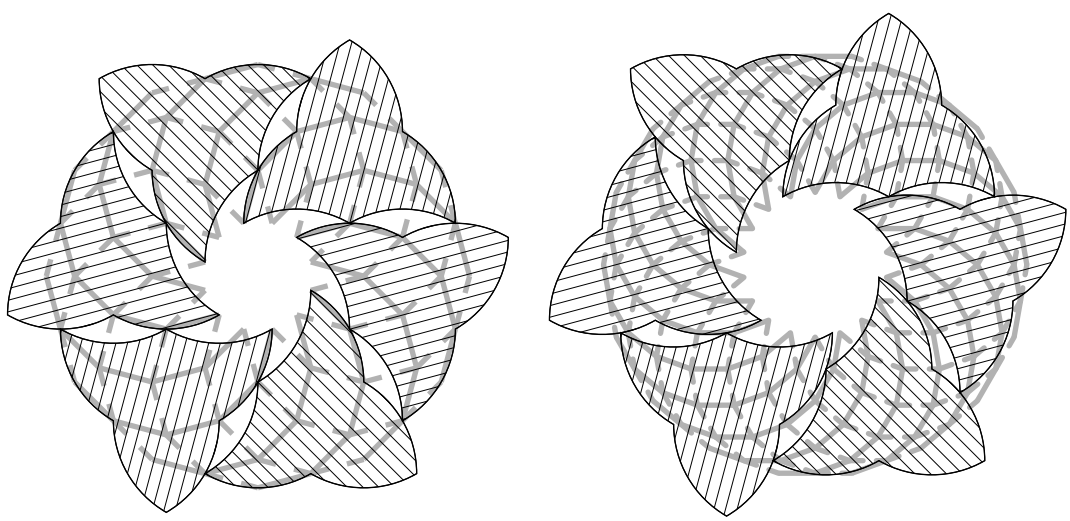

Figure 5.5: 6 cover elements on structures with configurations 12;5 and 18;7

5.2.1 Plates with straight boundaries

The wedge shaped cover elements found using the method of inclination lines, Section 3.3, have the property of always subtending an angle equal to α. As angulated elements with more than *three* bars or joints of finite size subtend angles larger than α, the wedge solution cannot readily be used for plate elements. However if the wedges are not positioned so that their tips coincide with the origin the wedge solution can be used.

If the underlying angulated element has *three* or fewer bars the position of the wedges in relation to both the overall structure and the joints can be found as the position will satisfy a number of geometrical conditions. From Figure 5.6:

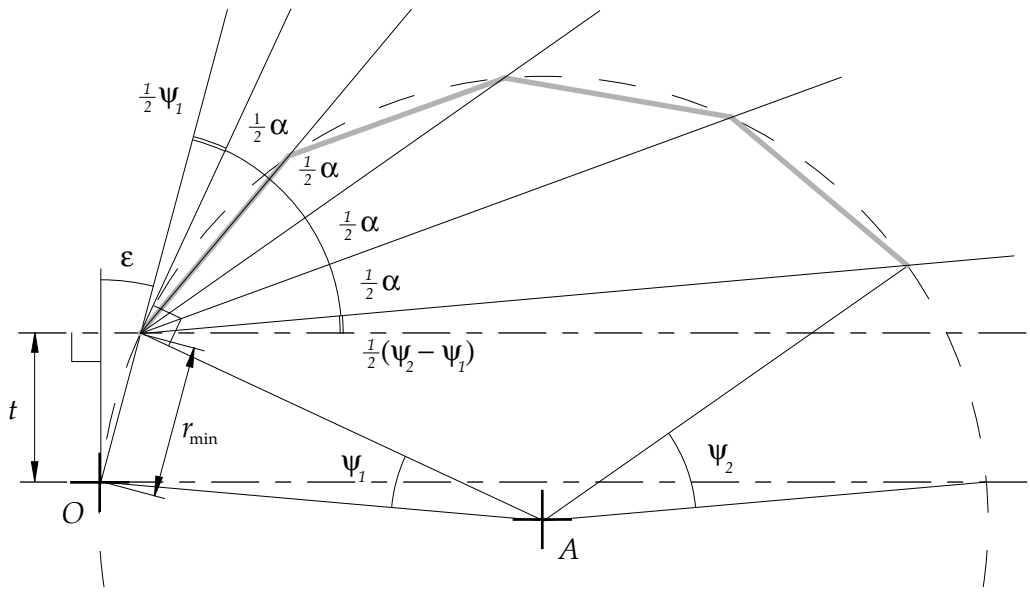

Figure 5.6: The distance t is a function of n, k, ψ_1 and ψ_2

$$\varepsilon = \frac{\pi}{2} - \frac{\psi_1}{2} - k\frac{\alpha}{2} - \left(\frac{\psi_2 - \psi_1}{2}\right) = \frac{\pi}{2} - k\frac{\alpha}{2} - \frac{\psi_2}{2} \tag{5.8}$$

And:

$$t = r_{min} \cos \varepsilon \tag{5.9}$$

Using Equations 1.1 and 2.14:

$$
\begin{aligned}
t &= 2r^\star \sin\left(\frac{\psi_1}{2}\right)\cos\left(\frac{\pi}{2} - k\frac{\pi}{n} - \frac{\psi_2}{2}\right) \\
&= 2r^\star \sin\left(\frac{\psi_1}{2}\right)\sin\left(k\frac{\pi}{n} + \frac{\psi_2}{2}\right)
\end{aligned} \tag{5.10}
$$

From Figure 5.7:

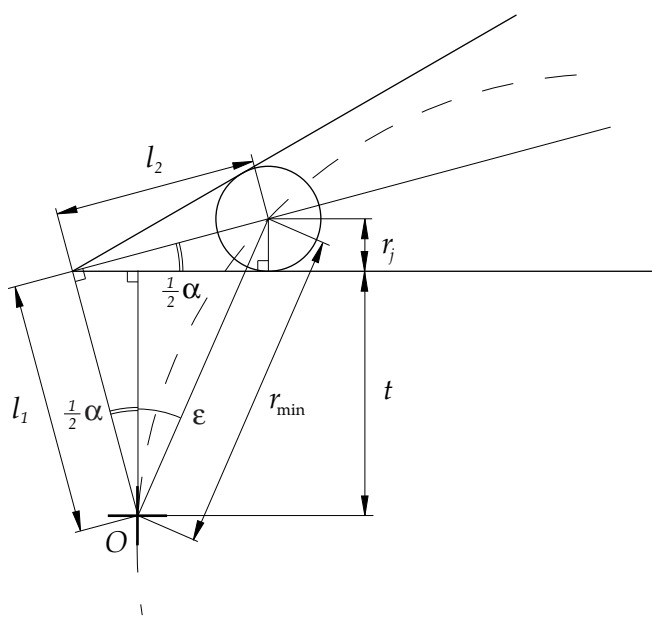

Figure 5.7: Wedge position for plates with straight boundaries

$$
l_1 = \frac{t}{\cos\left(\frac{\alpha}{2}\right)} \tag{5.11}
$$

$$
l_2 = \frac{r_j}{\sin\left(\frac{\alpha}{2}\right)} \tag{5.12}
$$

Using Equations 2.14 and 5.8:

$$
\begin{aligned}
r_j + t &= r_{min}\cos\varepsilon \\
\frac{t}{r^\star} &= 2\sin\left(\frac{\psi_1}{2}\right)\sin\left(k\frac{\alpha}{2} + \frac{\psi_1}{2}\right) - \frac{r_j}{r^\star}
\end{aligned} \tag{5.13}
$$

Solutions for t must also satisfy the following equation, from Figure 5.7:

$$
r_{min}^2 = l_1^2 + l_2^2 \tag{5.14}
$$

Solving Equation 5.13 numerically, using r_j and ψ_1 as variables, the solutions of Equation 5.14 can be plotted. As both $n; k$ are present in the equations, their values need to be chosen before any solutions can be found. The solutions shown in Figures 5.8 and 5.9 are for $n = 12$ and with $k = 2$ and $k = 3$. However, for small values of r_j and ψ_1 the algorithm used did not give valid solutions and therefore the results for $r_j/r^\star \leq 1\%$ not usable.

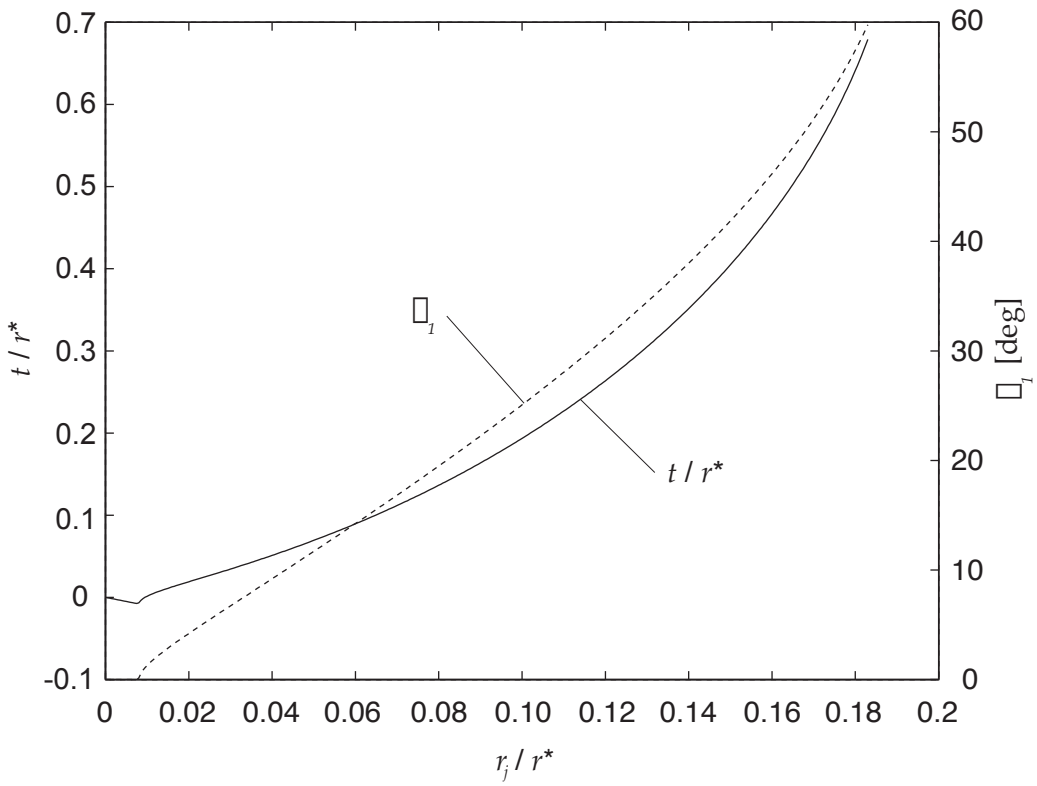

Figure 5.8: For $n;k = 12;2$, t and ϕ_1 as a function of r_j

For configurations with *four* or more bars the angulated element subtends an angle larger than α. Therefore joint j_1 must be positioned a distance from the tip of the wedge. For $k = 4$, the length of r_{min} can be found using Equation 2.14 and from Figure 5.11 to obtain:

$$r_{min} = l\frac{\sin\frac{\alpha}{2}\sin\left(\frac{\pi}{2} - \frac{\alpha}{2}\right)}{\sin\alpha\sin\left(\frac{\alpha}{2} + \varepsilon\right)} \tag{5.15}$$

By evaluating these two equations numerically, using ψ_1 as the variable, configurations for which Equations 2.14 and 5.15 are equal can be calculated. It was found that only configurations with $n \geq 12$ can have wedges positioned over them.

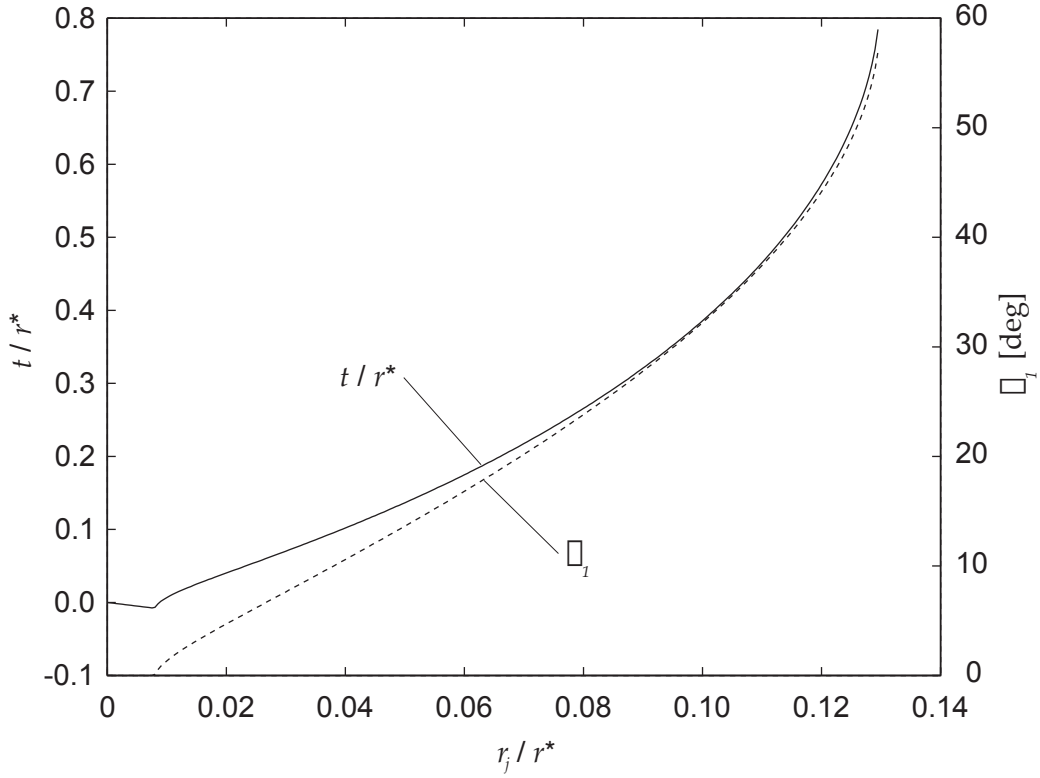

Figure 5.9: For $n;k = 12;3$, t and ϕ_1 as a function of r_j

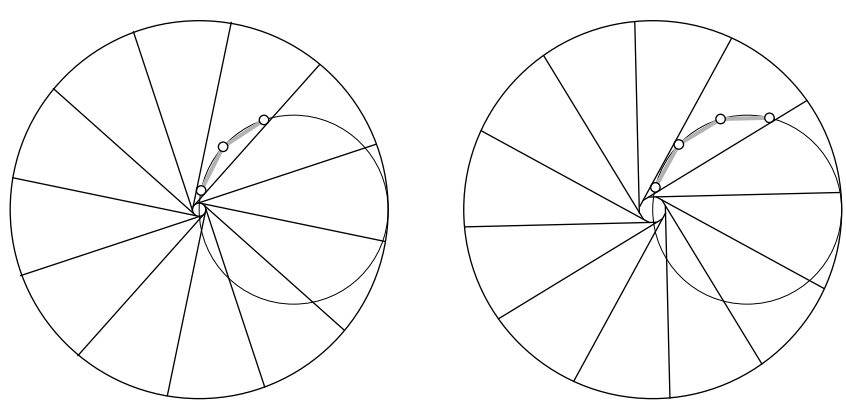

Figure 5.10: Design of wedge shaped plates with $k = 2$ and $k = 3$

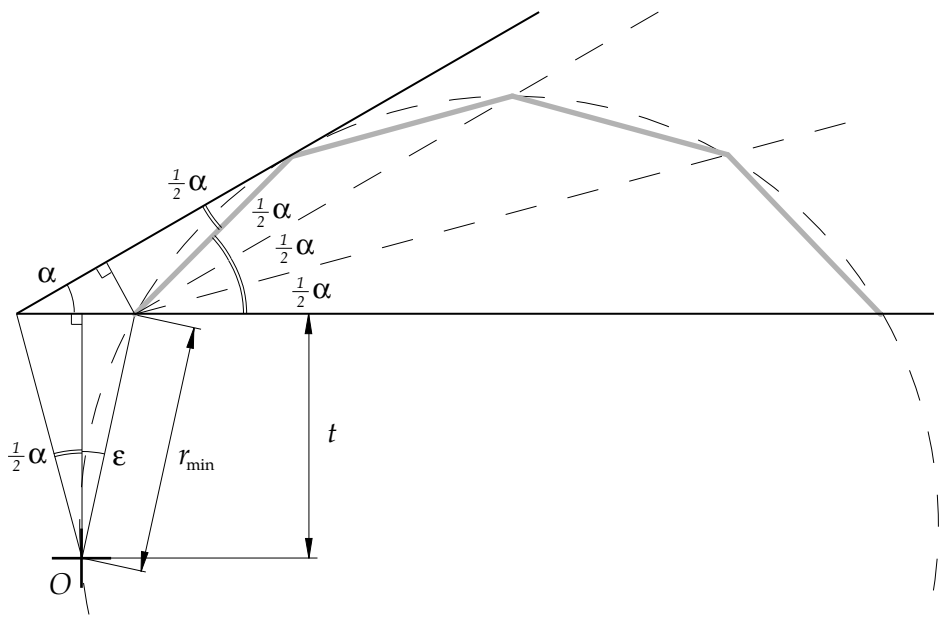

Figure 5.11: Wedge position for plates with straight boundaries

The joint size can be introduced into Equation 5.5 by equating the length $l^\star$ and β from Figure 5.12. Equation 5.15 is thus modified to:

$$r_{min} = l^\star \frac{\sin\beta \sin\left(\frac{\pi}{2} - \frac{\alpha}{2}\right)}{\sin\alpha \sin\left(\frac{\alpha}{2} + \varepsilon\right)} \tag{5.16}$$

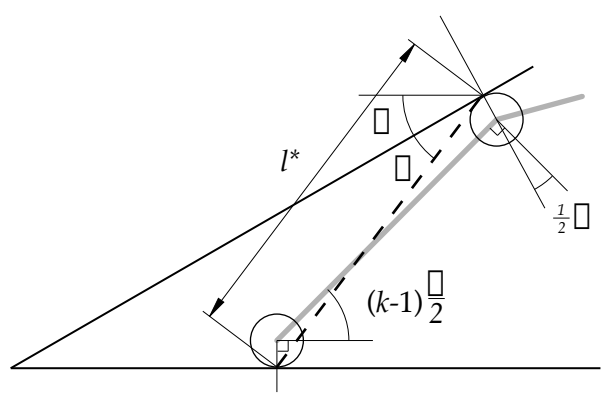

Figure 5.12: Effect of joint size on position of wedge for $k = 4$

The results for $n; k = 12;4$ are plotted in Figure 5.13.

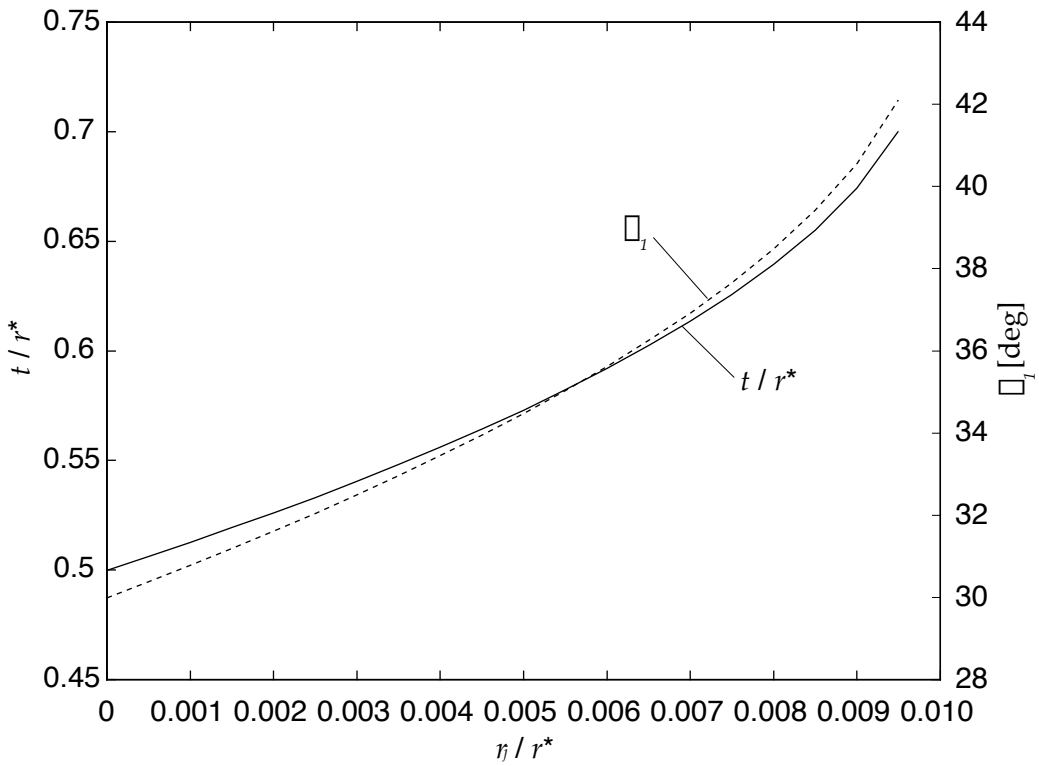

Figure 5.13: For $n;k = 12;4$, t and ϕ_1 as a function of r_j

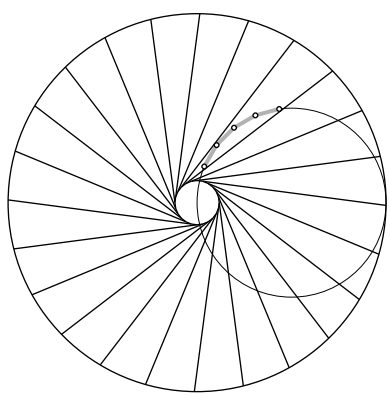

Figure 5.14: Design of wedge shaped plates with $k = 4$

5.2.2 Plates with non-straight boundaries

Using non-straight boundaries it is possible to design structures with a circular opening, as described in Section 5.1.3, and to minimize the gap, at the centre of the structure, that resulted from using plates with straight boundaries.

The design of this type of structure is an iterative process based on trial and error as there is a large number of variables which determine the final shape of the structure. Below is outlined a possible approach.

Using the design diagrams from Chapter 2 the configuration of the structure can be determined for a given set of requirements. Due to the presence of the joints in the plates, minimum values for the reduction angles can be found from Equation 2.20 and therefore an estimated joint size is required before starting. Using Figure 2.13 the maximum reduced angle of rotation can be found. From the same diagram it is possible to find an equivalent configuration with an unreduced angle of rotation equal to the reduced angle of rotation previously obtained. The equivalent configuration should be chosen so that k is a positive integer while n can be any positive number, not necessarily an integer. Using this equivalent configuration it is possible to evaluate the performance of the structure in the other diagrams as the equivalent configuration will have the same performance as the present structure.

When a configuration has been chosen, it is possible to determine the limits to the boundary and thus create a design template similar to Figure 4.7. If a circular opening is a design criterion, the configuration must satisfy Equation 5.6. If this is satisfied the radius of the opening can also be defined in the design template. The inclination of the inclination line is then found from Equation 3.31 and creating a number of triangular wedges, each subtending an angle α. The templates are then positioned along the inclination lines to set the limits for possible shape variations creating a wedge template.

If a graphical method is used, then the wedge template can be used as an overlay on a bar structure in the closed position. The inclination of the wedge is predetermined by the inclination angle but it is possible to vary the distance t as described in Section 3.5.1 and, following Equation 3.32, the distance s. One inclination line of the wedge will be shifted $2s$ along the other inclination line, as shown in Figure 5.16, but the limits for the two inclination lines are unchanged relative to their respective inclination lines. If t is equal to *zero* then there will be no opening at the centre of the structure and for t larger than zero, the central opening can be closed by modifying the shape of the boundary of the plate locally as described in Section 3.5.1.

If it is not possible to find a shape of the boundary of the plates that satisfies the required conditions, the process can be repeated with different values for the reduction angles, joint size or a different configuration.

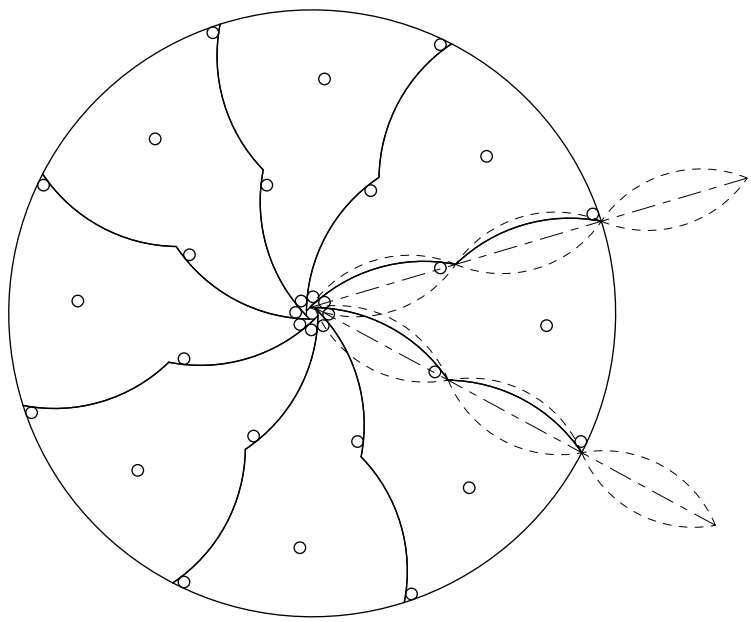

Figure 5.15: Use of wedge template to create allowable changes in the shape of the plates

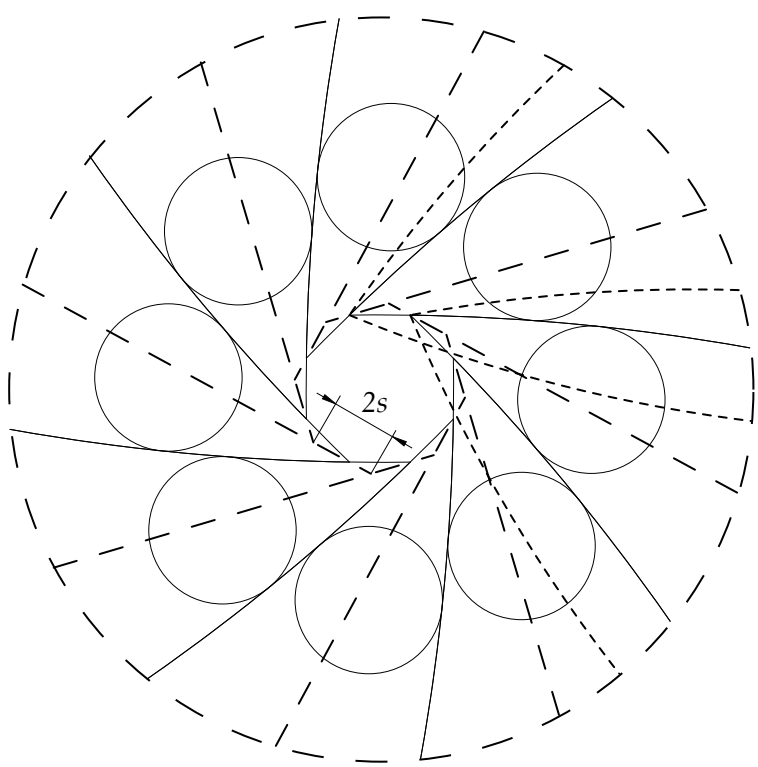

Figure 5.16: Shift of inclination lines and limits at the central opening

5.3 Physical models

Two physical models have been built to demonstrate the plate structures described above. Both of these have been designed using periodical boundaries with arcs of a predetermined radius. They were constructed from spark-eroded, 16 gauge Al-alloy plate. The joints were made from plastic snap rivets.

The first model built was built to demonstrate that it is possible to design plate structures without reducing the angle of rotation. To avoid the problems of contact between the joints and reduction of the rotation angle, joints j_1 and j_{k+1} were removed from the model, giving $\psi_{tot} = 0$. The structure was based on $n; k = 12; 4$ and the boundary was defined with arcs of radius $r^\star + r_j$ with $r_j/r^\star = 1.80\%$. The model is shown in Figure 5.17.

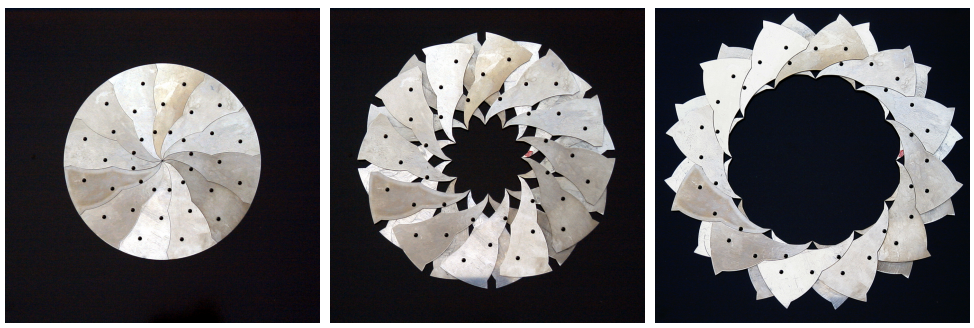

Figure 5.17: First model of plate structure

The second model was built with fewer elements, to show the possibility of forming a circular opening when the structure is in the open position. As with the first model, the design was based on arcs with radius $r^\star + r_j$. However, no joints were removed and therefore the reduction angles had to be found. This was done from Figure 5.18 and a design chart was plotted for this special case where the circular arcs have the radius $r^\star + r_j$. The reduction angles are given from Equation 5.17 and the design diagram is shown in Figure 5.19. The ratio $r_j/r^\star = 1.85\%$ forms a nearly circular central opening for $n; k = 12; 3$. The model is shown in Figure 5.20.

$$\psi_1 = \psi_2 = \arccos\left[\frac{\sin^2\left(\frac{\pi}{n}\right) - \frac{r_j}{r^\star} - \left(\frac{r_j}{r^\star}\right)^2}{\sin\left(\frac{\pi}{n}\right)}\right] - \frac{\omega}{2} \tag{5.17}$$

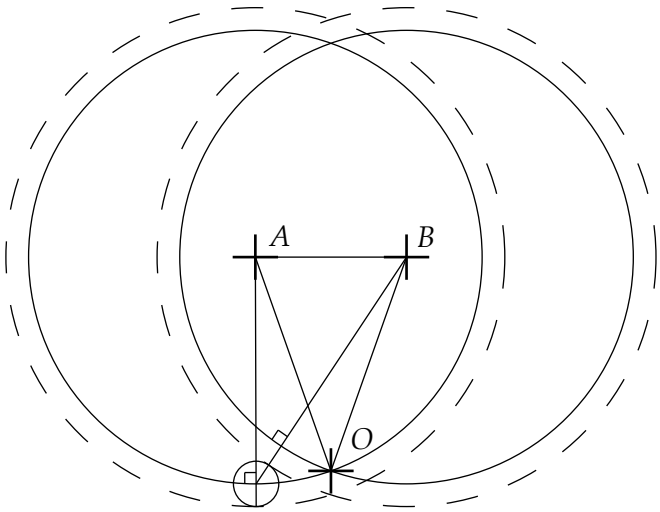

Figure 5.18: ψ_1 found for arc radius of $r^\star + r_j$

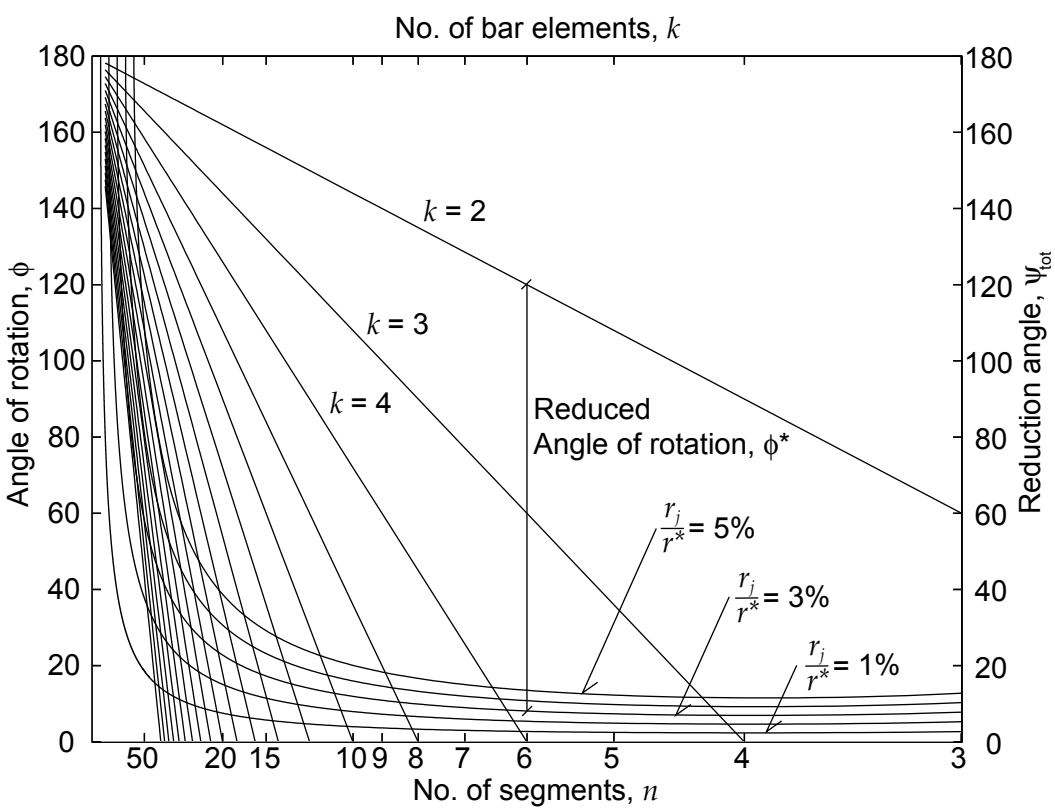

Figure 5.19: Reduced angle of rotation for various joint sizes

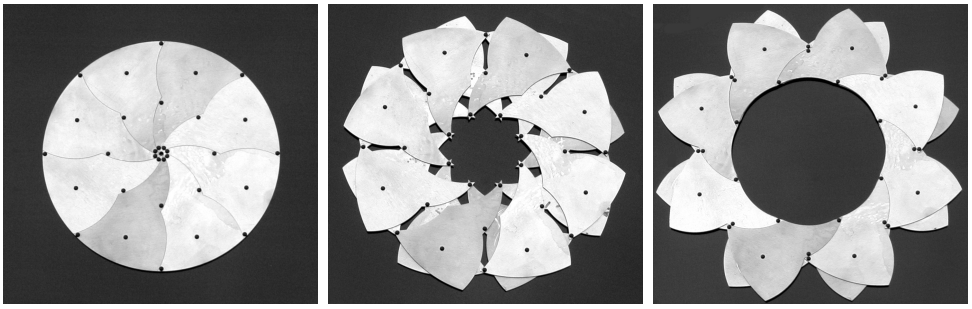

Figure 5.20: Second model of plate structure

Chapter 6

Discussion and Conclusion

This report has described the progress made so far in the development of design methods for covered bar structures for retractable roofs. It has been found possible to cover the bar structure with rigid elements and it has also been shown that it is possible to design structures made from rigid plate elements alone. In the sections below the possibility of using these solutions for retractable roofs will be discussed together with the application of the results and design approach presented in this report.

6.1 Solutions for Plate Shapes

It has been found that it is possible to design a large variety shapes for elements that cover the bar structure. All designs are based on a simple wedge shape.

The variety in the possible solutions enables this type of structure to accommodate a large variety of design criteria. Kassabian [7] showed that the simple wedge shaped solution could also be applied to structures of elliptical shape. However the solution did not give a continuous, i.e. gap free, surface in the open position. The analytical approach of considering the motion of neighbouring angulated elements, presented in this report, might provide solutions to this problem.

The analytical approach that has been developed has made it possible to develop a type of structure made solely from rigid plate elements. This solution does not rely on a bar structure and is therefore simpler and less expensive than structures requiring both angulated and cover elements. However, they have a reduced rotation angle and therefore smaller opening and stowage ratios.

The plate structures open the possibility of using this type of retractable structures for simple and inexpensive products. As there are no conditions on the outer shape of the structure, there are many possible shape variations, both in the open and closed positions.

6.2 Design Approach

The design methods described in Chapter 5 have proven to be a simple and strong tool for finding the overall shape of the structure. However, as there are a large number of design parameters some iteration is still needed to finalize a design.

In particular if the shape is to be optimised with respect to minimising the central opening in the closed position, while also minimising the distance from the joints to the boundary of the elements, this involves varying the position of the limits along the inclination lines and also possibly redefining the reduction angles and thus the limits themselves.

As this work is laborious to do manually, it would be useful if it could be automated. The method can possibly be programmed without extensive modification of the approach used, as there are only few variables which are not known once the overall configuration has been decided upon.

Though the proposed design approach cannot be considered to be exhaustive it still offers an insight into the possibilities of this type of structures which will form the basis for more complicated three-dimensional problems.

6.3 Future work

For these types of structures to become usable for retractable roofs, several key issues need to be resolved.

For the structure to be able to carry forces efficiently some sort of *three*-dimensional shape must be achieved. Also, using a flat roof creates durability problems especially in form of water run-off. There appear to be two approaches to this issue.

One is the approach proposed by Kassabian where the *two*-dimensional flat structure is projected onto a *three*-dimensional surface of some shape [7]. However, as observed in the model pictured in Figure 1.13 vertical gaps will often result from this approach as the vertical height will vary along the boundary of the cover elements. Thus, when the shift occurs, two boundaries in contact might have different vertical positions and thus a vertical gap will be present.

Another approach would be to define the mechanism of the bar structure on a *three*-dimensional surface instead of a plane. This approach is likely to be the more difficult of the two as a new mechanism will have to be derived whereas for the first approach, the basic concept is understood.

The support conditions for the structure will also have to be resolved. Kassabian [7] has done work on this subject, but the proposed solution might not be the most suitable for a retractable roof.

As mentioned above, solutions for non-circular structures would also have to be developed as these seem to provide the best possibilities for providing covering for the often non-symmetric stadia. However, newer stadia are being designed with a heavy emphasis on optimum viewing for the spectators. This produces circular shapes for most sports and therefore even the circular solutions presented in this report would provide an interesting possibility for future designs of stadia.

The possibility of creating circular or other shapes for the opening is also attractive as conventional rectangular designs for stadia are increasingly encountering problems with satisfying the need for good covering of the spectators and sufficient sun light and fresh air for the playing surface. The circular or near-circular opening would allow designers to make optimum use of the path of the sun [3, 9, 11, 12].

Bibliography

[1] Barnes, M., and Dickson, M. *Widespan Roof Structures*, First ed. Thomas Telford Publishing, London, 2000.

[2] Escrig, F., and Brebbia, C. *Mobile and Rapidly Assembled Structures II*, First ed. Computational Mechanics Publications, Southhampton, UK, 1996.

[3] Geraint, J., and Sheard, R. *Stadia: a design and development guide*, Third ed. Architectural Press, Oxford, UK, 2001.

[4] Hoberman, C. Reversibly expandable doubly-curved truss structure. USA Patent no. 4,942,700, 1990.

[5] Hoberman, C. Radial expansion/retraction truss structures. USA Patent no. 5,024,031, 1991.

[6] Ishii, K. *Structural design of retractable roof structures*, First ed. WIT Press, Southampton, UK, 2000.

[7] Kassabian, P. Investigation into a type of deployable roof structure. Final-year project, University of Cambridge, Engineering Department, 1997.

[8] Kassabian, P., and Pellegrino, S. Retractable roof structures. *Proceedings Institution of Civil Engineers Structures & Buildings 134* (Feb 1999), 45–56.

[9] Murray, C. *Stadium roofs*, First ed. The Sports Council, London, UK, 1995.

[10] Pellegrino, S., and You, Z. *Space Structures 4*, vol. 1. Thomas Telfford Publishing, London, 1993, ch. 84, pp. 783–792.

[11] Shields, A., and Wright, M. *Arenas: a planning, design and management guide*, 1995 ed. The Sports Council, London, UK, 1995.

[12] Thompson, P., Tolloczko, J., and Clarke, J. *Stadia, Arenas & Grandstands*, First ed. E & FN Spon, London, UK, 1998.

[13] You, Z., and Pellegrino, S. Foldable bar structures. *International Journal of Solids and Structures 34*, 15 (1997), 1825–1847.